

Consistent assignment of the vibrations of symmetric and asymmetric *para*-disubstituted benzene molecules

Anna Andrejeva, Adrian M. Gardner, William D. Tuttle and Timothy G. Wright^{a,*}

^aSchool of Chemistry, University of Nottingham, University Park, Nottingham, NG7 2RD, U.K.

*To whom correspondence should be addressed. Email: Tim.Wright@nottingham.ac.uk

Abstract

We give a description of the phenyl-ring-localized vibrational modes of the ground states of the *para*-disubstituted benzene molecules including both symmetric and asymmetric cases. In line with others, we quickly conclude that the use of Wilson mode labels is misleading and ambiguous; we conclude the same regarding the related ones of Varsányi. Instead we label the modes consistently based upon the Mulliken (Herzberg) method for the modes of *para*-difluorobenzene (*p*DFB). Since we wish the labelling scheme to cover both symmetrically- and asymmetrically-substituted molecules, we apply the Mulliken labelling under C_{2v} symmetry. By studying the variation of the vibrational wavenumbers with mass of the substituent, we are able to identify the corresponding modes across a wide range of molecules and hence provide consistent assignments. Particularly interesting are pairs of vibrations that evolve from in- and out-of-phase motions in *p*DFB to more localized modes in asymmetric molecules. We consider the *para* isomers of the following: the symmetric dihalobenzenes, xylene, hydroquinone, the asymmetric dihalobenzenes, halotoluenes, halophenols and cresol.

Keywords: Frequencies; Ground state; Substituted benzenes.

I. INTRODUCTION

Because an understanding of the trends in the vibrational spectroscopy and dynamics of molecules is linked to being able to refer to the same vibrational motions (normal modes) across species, it is desirable to label these in as consistent a manner as possible. In this way, when referring to a labelled vibration in one molecule, one can be sure of talking about the same vibration in a different molecule.

Since there are a whole range of substituted benzenes, it has been very common to refer to the phenyl-ring-localized vibrations of any such molecule in terms of the vibrations of the parent benzene molecule via the Wilson labelling scheme [1]. In previous work on the monosubstituted benzenes it has been noted by our group [2] and others [3,4] that in fact the use of the Wilson labelling scheme is fraught with uncertainty owing to the large differences between the forms of the normal modes of benzene and those of the monosubstituted species; this difference occurs even for the substitution of H for D in monodeuterated benzene [2]. This has been recognized by many workers, perhaps most notably Varsányi [5], who attempted to bring consistency to the labelling by proposing Wilson-type labels for a whole range of substituted benzenes; unfortunately, however, this was hampered by incomplete data sets, and there was also inconsistency concerning the employed labelling for molecules that contained “light” and “heavy” atoms; hence there are still numerous anomalies. We have previously noted this in Ref. [2] and in recent work on the electronic spectroscopy of the monohalobenzenes [6,7,8], where Varsányi’s suggested labels for the normal modes of fluorobenzene were different to those of the heavier species, even when the motion was very similar. In Table 1 we have given Varsányi’s assignments of the *p*-difluorobenzene (*p*DFB) and *p*-dichlorobenzene (*p*DCIB) vibrations, and although there is predominantly consistency across the a_2 , b_1 and b_2 modes, the ordering of the a_1 modes is significantly different. We also note that denoting the lowest wavenumber b_2 vibration as ν_{15} is consistent with Varsányi’s assignments for chlorobenzene, but not fluorobenzene [2,6,7]. In addition, and as will be discussed below, in many cases the assignments do not match the motion as determined using a Duschinsky approach, and indeed in a number of cases there is no clear Wilson mode with which to identify the vibration.

One possible way forward would be to use Mulliken labelling [9] (sometimes called Herzberg labelling [10]), whereby the normal modes are simply separated into symmetry blocks (in a predetermined order) and then to order them within these by wavenumber, with the highest first. This does, indeed, lead to a systematic and facile attribution of a mode label; however, it means that if the symmetries of two molecules are different and/or if the substituent itself contributes vibrations, then the label for a particular normal mode will alter from molecule to molecule making trends in vibrational wavenumber and activity difficult to see. However, there is a simple way forward: in Ref. [2] we noted that although there were stark differences in normal modes on moving from benzene- h_6 to monodeuterated benzene, and continued changes with the mass of the substituent beyond that, there

was very little further change if the substituent's mass was 15 amu or greater. On the grounds that fluorobenzene was the simplest type of monosubstituted benzene with a substituent mass ≥ 15 , we adopted the Mulliken labelling of the fluorobenzene normal modes, labelled M_i , for all monohalobenzenes. Further, for any substituent that had more than one atom and so would be contributing vibrations, such as CH_3 in the toluene molecule, we separated the substituent-localized vibrations from the list, so that the thirty phenyl-ring-localized normal modes constitute the M_i vibrations. These are usually easily identified, but also, as we showed in Ref. [2], by taking the calculated force field for fluorobenzene and artificially changing the mass of the fluorine atom to the combined mass of any substituent (e.g. to 15 for toluene), then very good approximations to the ring-localized mode wavenumbers can be obtained, and so the modes identified. Finally, calculated vibrational modes can then be cross-checked against visualizations and comparisons made to those of fluorobenzene (presented in Ref. [2]).

The question then arises as to whether the same labelling scheme can be applied to other families of substituted benzenes or, if not, whether similar schemes will work. In the present work we target the *para*-disubstituted benzenes, with *ortho* and *meta* versions left until a later date. We will examine the S_0 normal modes for a range of substituents, both symmetric ($p\text{-C}_6\text{H}_4\text{X}_2$) and asymmetric ($p\text{-C}_6\text{H}_4\text{XY}$). We shall initially consider how the Wilson modes of benzene evolve into those of the *p*DFB species. Following that, we shall consider how the M_i modes of fluorobenzene (FBz) are related to those of *p*DFB, and then how the *p*DFB modes evolve as the halogen mass changes for symmetric ($p\text{-C}_6\text{H}_4\text{X}_2$) and asymmetric ($p\text{-C}_6\text{H}_4\text{XY}$) cases. It will be concluded that it is indeed possible to label the vibrations consistently across a wide range of substituents based on the *p*DFB vibrations.

II. COMPUTATIONAL DETAILS

All of the harmonic vibrational frequencies were obtained using B3LYP/aug-cc-pVTZ calculations via the GAUSSIAN 09 software package [11]. For bromine and iodine atoms, the fully relativistic effective core potentials, ECP10MDF and ECP28MDF respectively, were used with corresponding aug-cc-pVTZ-PP valence basis sets. All of the calculated harmonic vibrational wavenumbers were scaled by the usual factor of 0.97 as an approximate method of obtaining anharmonic wavenumber values. We note that in our recent work on toluene [12,13] we found that these scaled harmonic values were at least as reliable as the explicitly calculated anharmonic values (with the latter being very expensive to calculate). In addition, in our previous work on the monohalobenzenes [6,7,8] our calculated scaled harmonic frequencies, except for a few low wavenumber vibrations, matched the reported experimental results well.

In the following we shall make use of vibrational wavenumbers calculated for the actual molecule, which we shall refer to as “explicit”, and also vibrations that are calculated using one molecule’s force field, but then artificially changing the mass of one or two atoms (referred to as artificial isotopes in the below) to match those of substituents (atomic or otherwise), which we shall refer to as “iso”. In this way we can map out changes in the vibrational wavenumbers that occur solely from the mass effect. In addition, we shall calculate generalized Duschinsky matrices using FC-LabII [14].

III. ASSIGNMENT OF THE S_0 VIBRATIONAL MODES of p DFB

We have already shown in previous work that the benzene Wilson modes are very different to those for monofluorobenzene (FBz) [2]: this is not so surprising as the normal modes will naturally need to change to compensate for the motion of a fluorine atom instead of a hydrogen. In a generalized Duschinsky picture, one can view the vibrations of FBz as mixed versions of the benzene Wilson modes, and this indicates that it is not always straightforward to make a 1:1 correspondence between a vibration of FBz and a Wilson mode of benzene from calculated vibrational mode diagrams [2,3,4]. Indeed attempting such a process for substituted benzenes has led to much frustration to workers in this area over the years. We thus anticipate that there will be significant differences between the vibrations of benzene and the corresponding *para*-disubstituted molecule, p DFB, and also between FBz and p DFB. In particular, in p DFB the motions of the fluorine atoms can be “in-phase” or “out-of-phase”, with these requiring different displacements of the other atoms, in order to keep the centre of mass stationary in each normal mode; conversely, if the vibration is such that the fluorine atoms are not moving, then we expect the motion and vibrational wavenumber to be similar in all three molecules.

For the cases where the substituents are both atomic, then the symmetric *para*-substituted benzenes ($pC_4H_4X_2$) have D_{2h} symmetry; however, since we wish the labelling scheme to cover asymmetrically-substituted molecules (pC_6H_4XY) as well, we employ C_{2v} symmetry throughout. As we noted, we shall also be able to establish the vibrational labelling of the phenyl-ring-localized vibrations for non-atomic substituents by “artificial isotope” (“iso”) calculations, mentioned above. For all cases in the present paper, we place the molecule in the yz plane, and the z axis runs through the two substituent atoms (or through each of the atoms of the substituents that is directly bonded to the phenyl ring). This means we separate the vibrations into $11a_1 + 3a_2 + 6b_1 + 10b_2$ groupings by symmetry, and this will be the case for both symmetrically- and asymmetrically-substituted molecules. Further, for molecules with a non-atomic substituent, such as a CH_3 group, the experimental and “explicit” calculation values will include modes that are substituent-localized: these do not form part of the labelled vibrations and must be treated separately; these are straightforwardly identified from their calculated vibrational motion.

In the following we shall first discuss how the *p*DFB modes are related to the Wilson modes and, as expected from our monosubstituted work, will conclude that the Wilson labels are not appropriate. We shall then look at whether the FBz vibrational labels, the M_i labels of Ref. [2], can be used to label the *para*-disubstituted vibrational modes; again, we shall conclude this is not possible. We shall then explore whether one can use the vibrational mode labels of *p*DFB for other symmetric and then asymmetrically *para*-disubstituted halobenzenes. We shall conclude that this is possible and shall then examine this labelling scheme finding that it also works well for *p*-xylene (*p*Xyl), hydroquinone (HQ), halotoluenes, *p*-cresol and halophenols.

A. Wilson labelling

In Figure 1 we show how the vibrational wavenumbers of benzene change as the masses of two *para*-related hydrogen atoms are varied from 1 to 19 amu simultaneously, keeping the force field constant. (Note that we have done the same plot with the force field of *p*DFB and varying the mass of the two fluorine atoms from 19 to 1 amu and get essentially the same picture.) On the left-hand side of the diagram we have labelled each mode with the Wilson labels, while on the right-hand side we have labelled the modes with a label, D_i , with the D representing “disubstituted” and i being determined by the Mulliken ordering of the vibrations of *p*DFB in the C_{2v} point group. We have separated the vibrations into C_{2v} symmetry groups in the plots, and have used the same symbol and line type for those pairs of vibrations that are connected to the same degenerate benzene mode, but which have a different symmetry in the C_{2v} point group. It is immediately seen that some vibrational modes are very mass dependent, falling dramatically with mass, while others are almost completely mass independent; in between there are others that have a significant but more subtle mass dependence. A number of the curves look like they undergo “avoided crossings”, a general feature that we noted for the monosubstituted benzenes in Ref. [2]. We interpret these in terms of the changing forms of the vibrations, which can loosely be thought of as mixing together as the vibrations become close together (i.e. in the region of a crossing, the normal modes look like superpositions of the motions of the two separated vibrations). We find that, after the avoided crossing, the vibrations gradually move back to their original form, but are now switched in energy: this is very reminiscent of the behaviour of avoided crossings for potential energy curves of diatomic molecules. In Table 1 we compare the normal modes of benzene by examining the overlap of their vibrational wavefunctions to those of *p*DFB *via* the calculation of a generalized Duschinsky mixing matrix. The magnitude of the Duschinsky matrix elements are indicated in Table 1 with the key that: if the mixing coefficient is > 0.5 , we denote this as a dominant contribution and employ bold text; a mixing coefficient between 0.2 and 0.05 is a minor contribution, and is listed within parentheses; contributions with a coefficient between 0.5 and 0.2 are listed as major contributions and listed with no parentheses; and contributions < 0.05 are ignored. If there are multiple major/minor contributions, they are listed in descending order of importance. In performing this comparison, we recall from Ref. [2] that several Wilson modes have

been misnumbered in various texts over the years, with the following switches often being required: 8a \leftrightarrow 9a, 8b \leftrightarrow 9b, 18a \leftrightarrow 19a, 18b \leftrightarrow 19b and 3 \leftrightarrow 14; where they have occurred, these misnumberings have been corrected in the present work. In Table 1 we also give the D_{2h} symmetries for each vibration. In Figure 2 we indicate the Duschinsky mixing coefficients by shading, to allow a quick visual assessment of the extent of mixing between the different vibrational modes.

We have also undertaken a comparison of the M_i modes of FBz with the D_i modes (see above) of p DFB. To do this we have first taken the force field for FBz and then calculated the wavenumbers as the mass of the *para* hydrogen has been increased from 1 to 19; again we maintain C_{2v} symmetry throughout and again we separate the vibrations into the four symmetry groups. We present the results graphically in Figure 3, where we have also included the variation in the wavenumbers of the vibrations from FBz to Bz – these parts of the plots are very similar to those shown in Ref. [2]. In Table 1 we have also indicated how the D_i and M_i modes are related to each other, in terms of generalized Duschinsky mixing.

In the following we shall discuss the trends of the vibrations in symmetry groups, from Bz \rightarrow FBz and from FBz \rightarrow p DFB; later we shall discuss previous assignments of the p DFB vibrations, as compared to the calculated values. We present the vibrational mode diagrams of the D_i modes of p DFB in Figure 4, which are in order of C_{2v} symmetry group and then by wavenumber, as discussed above.

1. a_1 vibrations

There are four high-wavenumber vibrational modes in benzene that transform as a_1 symmetry under the C_{2v} point group: these are the ν_2 , ν_{20a} , ν_{7a} and ν_{13} modes, given in order of their calculated wavenumbers. The explicit calculated wavenumbers for p DFB are given in Table 2, where it can be seen that there are only two high wavenumber vibrations, D_1 and D_2 , consistent with the fact that Figure 1 shows that two vibrations fall dramatically in wavenumber as we move from Bz \rightarrow p DFB via a symmetric mass change. Interestingly, when considering asymmetric mass changes, Figure 3 shows that one of these vibrations falls in wavenumber from Bz \rightarrow FBz, while one stays relatively constant, and then when the *para* hydrogen is subsequently changed in mass the other vibration falls in wavenumber from FBz \rightarrow p DFB. Helped by the results for monodeuterated benzene and FBz in Ref. [2], here we can establish that the two highest-wavenumber modes in p DFB have dominant contributions from Wilson modes ν_2 and ν_{13} , with the ν_{7a} mode losing its identity between Bz and FBz, while the ν_{20a} mode loses its identity between FBz and p DFB. Both ν_{7a} and ν_{20a} then appear only as non-dominant contributions to other p DFB vibrations (Table 1). (In a similar way, although the FBz modes M_1 – M_3 have major contributions from the three Wilson modes ν_2 , ν_{20a} and ν_{13} , the ν_{7a}

vibration has lost its identity and contributes to a number of the M_i modes [2,6].) With regard to the M_i modes, on moving from FBz \rightarrow to p DFB we find the M_2 mode loses its identity and only appears via non-dominant contributions to a number of D_i modes, as can be seen in Table 1. (The M_i mode diagrams are given in Ref. [2].)

It is very interesting to note that the four high-wavenumber modes of benzene, 2, 7a, 13 and 20a all have H motion at the *ipso* and *para* positions and so it might have been expected that all would fall in wavenumber as the mass of the corresponding “hydrogen” atoms were increased; however, the motions mix quite significantly (Figure 2 and Table 1) in forming the D_i modes resulting in the D_1 and D_2 modes having very little motion of these H atoms. A possible interpretation of this behaviour is that D_1 is made up of combinations of ν_2 and ν_{7a} , which respectively have in- and out-of-phase motions of these hydrogens and that these then cancel in forming D_1 , while the enhanced *ipso* and *para* motion of the other vibration formed upon substitution causes a stark falling in wavenumber, which is revealed by the ν_{7a} mode mixing with other a_1 vibrations, all the way down to D_{11} . A similar picture holds for the formation of D_2 from ν_{13} and ν_{20a} , this time resulting in contributions of ν_{20a} to vibrations down as far as D_{10} , and D_2 having a dominant contribution from ν_{13} (Table 1).

This picture also fits in with the mixings at the “intermediate” FBz stage (see Duschinsky mixings in Refs. [2,6]), where these four vibrations mix to form M_1 – M_3 , with respective dominant contributions from ν_2 , ν_{20a} and ν_{13} – the fourth resultant vibration falls strongly in wavenumber with the single substitution and results in contributions of ν_{7a} to a range of M_i modes all of the way down to M_{11} . The mode diagrams (see Ref. [2]) indicate that all three modes, M_1 – M_3 , have *para* position H motion, but again combinations of these form when moving from FBz \rightarrow p DFB to give rise to D_1 and D_2 , with dominant contributions from M_1 and M_3 , respectively; and the third vibration falls in wavenumber and leads to mixing of M_2 into D_i modes down to D_{11} (Table 1).

We now highlight the fact that the next two p DFB vibrations, D_3 and D_4 have dominant contributions from Wilson modes ν_{9a} and ν_{18a} and that these two vibrations are dominant contributions to modes M_4 and M_5 [2,6] consistent with the make-up of these two D_i modes (Table 1). Looking at Figures 1 and 3, we can trace these modes across the diagram noting that they appear to be crossed by other M_i and D_i modes as the masses increase, yet regain their identities after the crossings. The next two D_i modes, D_5 and D_6 are extremely mixed both in terms of Wilson or M_i modes; as such, these are vibrations that can only unambiguously be identified with their D_i labels. The D_7 mode has essentially the same motion as the Wilson mode ν_{8a} , or the M_7 mode of FBz, while the D_8 mode can be strongly associated with the Wilson ν_{19a} mode, or M_8 . Modes D_9 and D_{10} are heavily mixed in terms of both Wilson and M_i modes and so can only be unambiguously identified with their D_i label; D_{11} has a dominant contribution from Wilson mode ν_{6a} and it can also be associated with FBz mode M_{11} . (We note,

however, that the M_{11} mode becomes associated with Wilson mode ν_{7a} for the heavier monohalobenzenes [7,8].) Finally, it is interesting to note that D_5 and D_6 both have dominant contributions from M_6 ; additionally, D_9 and D_{10} both have dominant contributions from M_{10} . We have mentioned that M_2 loses its identity when moving from FBz to p DFB, and this is also true of M_9 , which provides major and minor contributions to a range of D_i modes.

The mixings for Bz \rightarrow p DFB can be seen in a more visual way in the Duschinsky matrix in Figure 2, while a similar figure and other discussion for Bz \rightarrow FBz has been presented in our earlier work [2,6].

a_2 vibrations

The three vibrations of a_2 symmetry, D_{12} , D_{13} and D_{14} have very similar atomic motion to the corresponding Wilson modes in benzene (ν_{17a} , ν_{10a} and ν_{16a}), none of which involve the substituted atoms; a similar picture holds when moving from FBz \rightarrow p DFB. This effect is exemplified in the close to horizontal line in the mass correlation diagrams for this symmetry block in Figures 1 and 3, which show that the vibrational wavenumbers are almost entirely mass independent. As such these modes can be described with any of the three labelling schemes discussed herein. The Duschinsky matrix in Figure 2 also shows this clearly.

b_1 vibrations

Wilson modes ν_5 and ν_{17b} appear to have in and out-of-phase, out-of-plane motion of the *ipso* and *para* hydrogens and these combine together to form the D_{15} and D_{16} modes in p DFB there is also mixing in of the ν_{10b} motion, which has a similar out-of-plane C-H motion as ν_5 , but these two vibrations have a different phase with respect to the motion of the other C-H groups. It is notable that the low-wavenumber ν_{11} vibration contributes to these vibrations (Table 1). A similar story holds for the M_{15} – M_{17} modes when the Wilson modes are considered for benzene \rightarrow FBz (Refs. [2, 6]) and it is thus unsurprising that when moving from FBz \rightarrow p DFB, we see that the D_{15} and D_{16} modes are mainly made up of those M_i modes. In summary, although D_{15} and D_{16} have dominant contributions from ν_5 and ν_{17b} , respectively, they have majority contributions from other modes and so will have differing motions from the Wilson (or M_i) modes.

The next four D_i modes, D_{17} – D_{20} , are interesting in that although they become mixed versions of the corresponding Wilson modes ν_{10b} , ν_4 , ν_{11} and ν_{16b} , with the three highest wavenumber ones having dominant contributions, although the ordering has changed as a result of avoided crossings that can be seen in Figure 3. Furthermore, the lowest wavenumber mode, D_{20} , has its largest (major) contribution from ν_{16b} , but this latter mode is also the dominant contribution to mode D_{18} . Thus, there is much mixing and wavenumber order change in these b_1 vibrations. In terms of the M_i labels a similar story holds, although we note that modes M_{16} and M_{17} do not appear as dominant contributors to any vibration, and so have largely lost their identity. It is interesting to note that the ν_4 vibration is a

dominant contribution to M_{18} which does not change much from Bz \rightarrow FBz; however, from FBz \rightarrow p DFB the M_{17} and M_{18} vibrations appear to involve in- and out-of-phase motions of the *para* hydrogens. These vibrations then mix when moving from FBz \rightarrow p DFB, with one resultant vibration, D_{17} , being largely independent of mass, while the other drops sharply and leads to the M_{17} vibration contributing to a range of D_i modes, down to D_{20} .

In summary, neither the Wilson nor M_i labels are appropriate for these vibrations, with D_{20} only being unambiguously identifiable with its D_i label. Finally, it is interesting to note that both D_{19} and D_{20} have dominant contributions from the FBz mode M_{20} , and that both M_{16} and M_{17} lose their identities upon moving from FBz to p DFB.

b_2 vibrations

The first four vibrations of b_2 symmetry, $D_{21} - D_{24}$, have motions that are very close to the corresponding Bz vibrations ν_{20b} , ν_{7b} , ν_{9b} and ν_{18b} (Table 1), and also close to the corresponding M_i modes (Refs. 2 and 6).

Modes D_{25} and D_{26} are also well described by Wilson modes ν_{15} and ν_3 , although the wavenumber ordering has swapped over. In terms of the M_i labels there are dominant and major contributions from M_{26} to these vibrations, respectively, while M_{25} only appears as non-dominant contributions to these (and other) vibrations. Each of M_{25} and M_{26} are made up of major contributions from ν_{15} and ν_3 , and during the FBz \rightarrow p DFB phase, these M_i modes mix and then largely resolve back to the original Wilson motion; albeit in the reverse order.

The next four modes, $D_{27} - D_{30}$ are less straightforward, with D_{27} and D_{28} having dominant contributions from Wilson modes ν_{14} and ν_{6b} , respectively, but these are not in the same wavenumber order as in Bz; indeed, the situation is a little more complicated as evinced in Figure 3. By making use of the FBz mixing results from Refs. [2 and 6] it can be seen that ν_{14} mixes with the ν_{8b} mode from Bz \rightarrow FBz to yield one mode that is relatively insensitive to mass changes in the *ipso* position, and this becomes the M_{27} mode that is largely ν_{14} ; the other mode, which is more mass sensitive, falls in wavenumber leading to further mixings of ν_{8b} as far down as M_{30} . This leaves M_{28} being dominated by ν_{19b} and M_{29} being dominated by ν_{6b} (see Refs. [2, 6]). When moving from FBz \rightarrow p DFB, M_{28} undergoes mixing with M_{27} , forming the D_{27} vibration, which is largely independent of mass changes in the *para* position, and is made up dominantly from the original ν_{14} Wilson mode, with an admixture of ν_{19b} . The other vibration appears to be largely composed of M_{27} , and whose behaviour hereafter is controlled by the ν_{8b} character, which continues to fall in wavenumber leading to interactions with the lower M_i vibrations and largely loses its identity; as a consequence, there are M_{27}/ν_{8b} contributions to

a number of vibrations (see Figure 3). The M_{29} mode largely retains its ν_{6b} character, becoming D_{28} after a flirtation with the M_{28} .

The two lowest modes D_{29} and D_{30} are mixed both in terms of Wilson or M_i vibrations, although it is notable that M_{30} is a dominant contribution to both of these, with each containing minor contributions from the M_{27} mode; however, there is no dominant contribution of the M_{27} mode to any D_i mode. The D_{29} vibration is the eventual resting place for the plunging ν_{8b} , although it has left behind contributions to other vibrations on the way. The D_{30} mode largely arises from the fact that M_{28} falls in wavenumber: with its dominant contribution from ν_{19b} , this leads to a major contribution from this vibration to D_{30} , although there are other major contributions from ν_{14} (via the interaction with M_{27}) and, surprisingly, ν_{18b} .

In summary, a number of the b_2 vibrations can be connected with a Wilson mode, although the ordering is not always as expected. Further, for some of these, the motion will be significantly affected by mixing, and in two cases the mixing is severe and these can only be unambiguously identified by their D_i label.

B. Trends in vibrational wavenumbers of $pC_6H_4X_2$ and assignment of vibrations

In Figure 5 we show the variation of the wavenumber for each of the D_i vibrations from 15 amu onwards with simultaneous variation of the mass of the two X substituents and indicated with the lines. (The symbols represent the experimental values and will be discussed further below.) These have been calculated by taking the force field of $pDFB$ and artificially changing the mass of the F atoms from 15 through to 127, with the lightest mass matching that of a CH_3 group and the heaviest matching that of the iodine atom. As may be seen, although there is some variation with mass, it is nothing like as stark as that found between Bz and $pDFB$ (Figure 1), and in particular there are no avoided crossings or evidence for large mixings or deviations of the vibrational motion. However the ordering of the explicitly calculated wavenumbers of D_5 , D_6 and D_7 do change with increasing mass of the halogen, which is not reflected in the isotopic wavenumbers of these vibrations. Along this series, we shall be interested in masses that correspond to those for p -xylene ($pXyl$), $pDFB$, $pDCIB$, p -dibromobenzene ($pDBrB$) and p -diiodobenzene ($pDIB$). In Figure 6 we show Duschinsky matrices for the vibrations obtained at these corresponding masses, with the comparison being with $pDFB$ in all cases. As may be seen, there is a strong diagonal nature to the matrices suggesting that the $pDFB$ vibrational motions will be close to those of the respective molecules, and so we can give the vibrations a D_i label accordingly.

In producing Figure 5 and Table 2, we had to assign the vibrational wavenumbers to the D_i modes, and we now discuss this briefly for each molecule. Previous assignments of the $pC_6H_4X_2$ spectra have

been in terms of Mulliken, Wilson and Varsányi labels, with the emphasis on the former. To aid the reader, we have included the D_{2h} Mulliken and symmetry labels for each of the D_i vibrations in Table 2, while in Table 1 the Varsányi labels have been included for p DFB and p DCIB.

1. *para*-difluorobenzene

We now look at the previous assignments of the vibrations of the S_0 state of p DFB, which may be viewed as the prototypical *para*-disubstituted benzene molecule and has been the subject of a number of spectroscopic investigations beginning in the early 1950s. Generally, the fundamental vibrational wavenumbers derived in the earlier studies are in good agreement with the most recent vapour-phase IR/Raman study by Zimmerman and Dunn in 1985 [15]. This paper also makes frequent reference to unpublished electronic spectroscopy results, which do not appear to have been published since then; although there is an earlier published fluorescence study of solid samples at 4 K by one of the authors [16]. The assignments in Ref. [15] largely confirm those made in earlier investigations, but several vibrational wavenumbers are reassigned and this work has been used as the key reference for the S_0 vibrational wavenumbers in later studies. Despite this, we believe several vibrational wavenumbers have been incorrectly assigned in Ref. [15]. The first of which is the vibrational wavenumber assigned to D_{24} (which is a b_{2u} symmetry mode, ν_{19} in Mulliken numbering). This vibration was assigned to a wavenumber of 1437 cm^{-1} in previous work [23], however Zimmerman and Dunn suggested that this could be incorrect if that feature corresponded to one they saw at 1431 cm^{-1} with the wrong band profile; on this basis they assigned a wavenumber of 1633 cm^{-1} to this vibration [15]. However, based on calculated vibrational wavenumbers, and through comparison with the wavenumber of this vibration in other *para*-disubstituted molecules (*vide infra*), we believe that this assignment is incorrect, while the original assignment fits well with our calculated wavenumber and trends across the series. Jarzęcki et al. [17] were also not convinced by the reassignment of the D_{24} wavenumber in Ref. [15] based on disagreement with their calculated vibrational wavenumber.

The wavenumber associated with the highest b_{2u} vibration, D_{21} , which in previous work and Table 2 of Ref. [15] was given as 3073 cm^{-1} , was given as 3091 cm^{-1} in Table 1 and the text of that work. We note that the value of 3091 cm^{-1} for this vibration is consistent with the corresponding value for p DCIB, but not with p DBrB, which is more in line with the lower value – our calculated values are not able to differentiate between these. (As is often the case, the assignment of the high wavenumber C–H stretch vibrations is fraught with uncertainty.) Also, the authors of Ref. [15] were of the view that a previous value of 1286 cm^{-1} for the D_{25} mode (Mulliken mode ν_{20}) was too low, and reassigned this as 1306 cm^{-1} on the basis of their IR measurements, this is consistent with the calculated wavenumber and trends across the series (see Table 2).

The wavenumber of the D_{12} vibration, which is of a_u symmetry in the D_{2h} point group and is expected to be both IR and Raman inactive, comes from a hot band in the two-photon electronic spectrum of Robey and Schlag [18] as tabulated and discussed in Ref. [15], and is confirmed in the later combined laser induced fluorescence and dispersed fluorescence study of Knight and Kable [19]. Only one new S_0 wavenumber value comes from that fluorescence study, where a value of 446 cm^{-1} is obtained for the D_{29} mode (Mulliken mode 27) – this had been estimated as 434 cm^{-1} in Ref. [15]. Additionally, a slightly refined value of 422 cm^{-1} is given for the D_{14} mode in Ref. [19].

2. *para*-dichlorobenzene

Where available, the experimentally-derived vibrational wavenumbers for *p*DCIB are taken from the gas phase IR study of Saėki [20], with the remainder from the IR and Raman study of Scherer and Evans [21] (also tabulated by Green [22]). These largely confirm the earlier assignments of Stojiljković and Whiffen [23], and we discuss some of the differences. (The reader is alerted to the fact that Scherer and Evans [21] and Green [22] each used different numberings of the vibrations, each different to the usual Mulliken ordering, as used by Saėki [20].) Stojiljković and Whiffen [23] observed a band at 1260 cm^{-1} in their IR spectrum, which they assigned to a b_{2u} fundamental vibration, corresponding to D_{25} . This was later reassigned by Scherer and Evans [21] to a combination band, who then assigned a band observed at 1221 cm^{-1} to this fundamental vibration. Because band profiles are not always an unambiguous indication of the vibrational symmetry [20] and because of the good agreement between our calculated vibrational wavenumber for the D_{25} vibration of 1264 cm^{-1} , and the 1260 cm^{-1} value of Stojiljković and Whiffen [23], combined with the expected trend of this vibration with mass (see Table 2), we favour the earlier assignment. A possible assignment for the lower wavenumber 1217 cm^{-1} band is the $D_{13}D_{14}$ ($815 + 410 = 1225\text{ cm}^{-1}$) combination, consistent with the assignment given to a band observed at 1219 cm^{-1} in the IR spectrum of Stojiljković and Whiffen [23]. It is noted that Saėki [20] assigned wavenumbers of 1393 cm^{-1} and 1417 cm^{-1} to vibrations which we deduce to be D_{25} and D_{24} , respectively; the lower wavenumber band appears to be the same IR band observed by Scherer and Evans [21] and Stojiljković and Whiffen [23], which was assigned to a b_{2u} fundamental, which we deduce is D_{24} , in good agreement with our calculated wavenumber of 1378 cm^{-1} and the expected mass trend (see Figure 5). As a consequence, the 1417 cm^{-1} assignment by Saėki to D_{24} must be incorrect.

We note at this point that the pseudo-Wilson assignments made by Varsányi [5] for *p*DCIB, which was classified as a *para*-di(“heavy”) molecule, results in several discrepancies in assignments when one attempts to compare to the vibrational wavenumber of *p*DFB, which was considered as a *para*-di(“light”) molecule (see Table 1). Similar discrepancies arose for the monohalobenzenes between FBz and the heavier chloro-, bromo- and iodo- analogues [7,8]. As a consequence we do not favour the Varsányi assignments.

3. *para*-dibromobenzene

The experimentally determined vibrational wavenumbers for *p*DBrB are summarized in Table 2. These are taken from the liquid phase IR spectra of Green [22], which are in excellent agreement with the earlier solution phase IR values of Stojiljković and Whiffen [23], from which remaining wavenumbers are taken from the solution phase Raman spectra where possible; the exception to this is the 1290 cm^{-1} value assigned to D_{26} taken from Herz et al. [24]. Also, Green [22] suggested a feature with a wavenumber of 1212 cm^{-1} be assigned to a fundamental, which corresponds to D_{25} , rather than the 1251 cm^{-1} assignment of Stojiljković and Whiffen [23] however, we favour the 1251 cm^{-1} assignment owing to the excellent agreement with our calculated wavenumber of 1260 cm^{-1} and the trend in the wavenumber of this vibration with mass (see Table 2). A possible assignment of the 1212 cm^{-1} feature is to the $D_{13}D_{14}$ ($815 + 402 = 1217 \text{ cm}^{-1}$) combination, consistent with the assignment of the feature at $\sim 1220 \text{ cm}^{-1}$ of *p*DCIB [23]. We also note that the value for D_{17} we employ was estimated by Green [22] to be 680 cm^{-1} , which is in excellent agreement with the calculated value.

4. *para*-diiodobenzene

The *p*DIB molecule is the least investigated of the symmetrical *para*-disubstituted species. The majority of the observed fundamental vibrations are taken from the solution phase IR/Raman study of Stojiljković and Whiffen [23], who also estimated several values based on the trends in wavenumbers observed for the lighter *para*-dihalobenzenes, with the value for the D_{30} vibration taken from the solution phase IR spectrum of Griffiths and Thompson [25]. The lowest wavenumber vibration of b_{3u} symmetry, D_{20} herein, is assigned to a weak feature observed at 105 cm^{-1} in the IR spectrum of Griffiths and Thompson (which shifts to 113 cm^{-1} upon cooling the sample to $-170 \text{ }^\circ\text{C}$) [25]. Although the calculated wavenumbers for this vibration are significantly lower than the experimental wavenumbers for both *p*DCIB and *p*DBrB, the discrepancy between this value, and the calculated value of 59 cm^{-1} , is notable. The calculated wavenumbers also suggest that this vibration should shift to lower wavenumber moving from *para*-dibromobenzene to *para*-diiodobenzene, indicating that this wavenumber should lie lower than the 103 cm^{-1} value of the former. Green [22] also notes that this value is higher than expected based on the trends in the wavenumbers assigned to this vibration for the symmetrical and non-symmetrical *para*-dihalobenzene molecules. As a result, we believe that the assignment of the 105 cm^{-1} feature to D_{20} is incorrect. (A possible assignment of this feature is to the $D_{29}-D_{30}$ ($255 - 144 = 111$) cm^{-1} difference band.) Finally, as with *p*DBrB, Green [22] favours a 1212 cm^{-1} assignment to the b_{2u} vibration (D_{25} in the present notation) that Stojiljković and Whiffen [23] assign to a feature observed at 1242 cm^{-1} in their IR spectrum. Again, we favour the assignment made by Stojiljković and Whiffen [23] based on the good agreement with our calculated wavenumber of 1252 cm^{-1} and the mass trend of this vibration. Lastly, we note that their estimated values for D_{14} , D_{17} and D_{29} are in good agreement with the calculated values.

5. *p*-Xylene

The vibrational wavenumbers for *p*-xylene are presented in Table 2, which have been taken from the vapour phase IR/Raman study of Draeger [26]. These values are generally in good agreement with previously reported values; however, a significant decrease is observed in the vapour phase wavenumber of 132 cm^{-1} we assign to D_{20} compared to the 152 cm^{-1} value determined from the liquid IR value [22]. The calculated values suggest that D_{25} has a lower vibrational wavenumber than that of D_{26} ; however, the experimentally derived wavenumbers assigned to these vibrations do not reproduce this trend, which were made based on the expected activities of these two vibrations under the assumption that *p*-xylene has D_{2h} symmetry [22,26]. We also note that Selco and Carrick²⁷ have recorded emission spectra of *p*-xylene following corona discharge with six vibrational wavenumbers reported. They compared their values to the earlier study of Green [22] and reasonable agreement is seen between those two sets of values and those calculated here, but there are two notable exceptions. Mode D_9 , for which Selco and Carrick [27] suggest a higher value of 842.3 cm^{-1} , in contrast to the lower value of 830 cm^{-1} from Draeger [26]; our calculated value cannot really distinguish between these, but we note that the higher value is close to the expected wavenumber for the $D_{11}D_{29}$ combination. Also, Selco and Carrick [27] suggest a higher value of 1656.7 cm^{-1} for the D_3 vibration, but our calculated value supports the lower value of 1616 cm^{-1} of both Green [22] and Draeger [26]. One possible assignment for the 1656.7 cm^{-1} band would be to the D_9^2 overtone band.

6. Hydroquinone (HQ)

There are not very many studies on the HQ molecule, but IR and Raman spectra in all three phases have been published. Varsányi [5] has attempted to label the vibrations; we find, however, that when compared to the calculated values a number of the wavenumbers cannot correspond to fundamentals and so we went back to both the original references cited therein, as well as more recent work. Varsányi [5] mainly made use of values in Hidalgo and Otero [28] and Jakobsen and Brewer [29], but there are other and more recent studies by Wilson [30], Fukushima and Sakurada [31], Kubinyi and Keresztury [32] and Kubinyi et al. [33] from which we have selected a close-to-complete set of experimental values that are both consistent with the explicit calculated values, but also fit in with the expected mass trends. These are given in Table 2 alongside the values for *p*Xyl and the symmetric *p*-dihalobenzenes. It has been deduced by Kubinyi et al. [33] that the most stable form of HQ is the *trans* form, which has C_{2h} symmetry; we thus include these symmetry labels in Table 2. We have favoured the gas-phase IR results of Wilson [30] where available, then the solution values (in benzene preferred over the CH_3CN ones) of Kubinyi et al. [33], followed by their solid-phase values; we occasionally use a solid-phase value from Kubinyi and Keresztury [32] or Jakobsen and Brewer [29].

We note that a value of 390 cm^{-1} has been associated with D_{29} previously [5,32]; however, this would be in poor agreement with our calculated value. A band was observed at 363 cm^{-1} (in benzene) and 377 cm^{-1} (solid), which is strong and Raman active; however, this was assigned as a b_g symmetry mode (in the C_{2h} point group for trans-HQ [33]) and so not assignable to D_{29} , which has a_g symmetry in C_{2h} . As a consequence, there is currently no wavenumber available for this vibration except our calculated value. The D_{22} wavenumber value may be very similar to the D_1 value, as it is for most of the substituted benzenes, but this is uncertain and so we have left this unassigned at the present time.

7. Mass correlation diagrams

With the assignments discussed above, and presented in Table 2, we can compare trends in vibrational wavenumbers, as is done in Figure 5. In this figure, we have plotted the artificial isotope (“iso”) values as lines, and experimental values as symbols. As may be seen, in almost all cases the agreement between the “iso” values and the actual experimental ones is extremely good; we recall that the agreement between the explicitly calculated values and experiment was also good (see Table 2). It is interesting to note that for the cases where there is some discrepancy between the “iso” values and the experimental ones, these correspond to the cases where the modes have a common dominant M_i contribution in FBz (see Table 1): M_{10} for D_9 and D_{10} ; M_{20} for D_{19} and D_{20} ; and M_{30} for D_{29} and D_{30} , each of which have dominant C–X motion. These motions are expected to be sensitive to any electronic structure changes induced by the substituent and thus, it appears that the force field changes enough from that of *p*DFB to give rise to vibrational wavenumbers that deviate visibly from the iso calculation, which assumes these are the same.

C. Asymmetrically substituted molecules, pC_6H_4XY

We consider three families of *para*-asymmetrically-disubstituted benzenes: the asymmetric dihalobenzenes, the halotoluenes and the halophenols. The tabulated experimental and explicitly calculated vibrational wavenumbers are given in Tables 3, 4 and 5, respectively.

We initially examine the asymmetric cases, pC_6H_4FX , where we keep one fluorine atom at mass 19, and vary the mass of the other, obtaining the lines plotted in Figure 7; we see that the variations are nowhere near as stark as those seen in Figures 1 or 3. (The symbols represent the experimental values and these will be discussed further below.) Additionally, the corresponding Duschinsky matrices are shown in Figure 8 and again show a strong diagonal nature. These points confirm that the D_i labels can be used for the asymmetric cases as well as the symmetric ones. In the above we have demonstrated that the “iso” wavenumbers obtained via the *p*DFB force field and artificial F isotopes give values that are largely in good agreement with the experimental values. In Table 3 we present the

“explicit” calculated and the experimental vibrational wavenumbers for the asymmetric (pC_6H_4XY) *para*-substituted dihalobenzenes and we shall now discuss the assignment of these. We have named these according to convention, with the halogens in alphabetical order, and then abbreviated in an obvious way, so that *pBrFB* represents *para*-bromofluorobenzene, for example.

1. $(X,Y) = \text{halogen}$

For *pClFB*, where possible, the vapour phase IR values of Narasimham et al. [34], are reported in Table 3. Where these are not available, the liquid phase IR values of Green [22] are employed. The wavenumbers obtained in IR/Raman studies of Patel et al. [35,36] are mostly in excellent agreement with these two earlier studies, except in the case of the wavenumbers previously assigned to modes D_{10} and D_{27} , which were concluded by Patel et al. [36] to originate from an impurity. We take the value of 639 cm^{-1} , determined from the vapour phase IR spectrum of Narasimham et al., [34] for D_{10} , which is in good agreement with the value of 630 cm^{-1} obtained by Patel et al. [36] and in significantly better agreement with our calculated wavenumber of 616 cm^{-1} for this mode than the 680 cm^{-1} value favoured in the earlier studies [22,34]. Based on the consistent wavenumber of 1086 cm^{-1} we have assigned to mode D_{27} for both *pBrFB* and *pFIB* (*vide infra*), a very similar value would be expected for this vibration in *pClFB*, and we therefore concur with the conclusion of Patel et al. [36] that the 1126 cm^{-1} assignment of Green [22] is likely erroneous, but they were not able to identify a new feature corresponding to this vibration. We have been unable to find an alternative wavenumber for this vibration in the literature and so adopt an estimated value of 1086 cm^{-1} for this fundamental based upon our calculated values, and the experimental values for the other fluorohalobenzenes (see Table 3). Finally the wavenumber assigned to D_9 is taken from the liquid phase Raman spectrum of Patel et al. [36].

The wavenumbers for *pBrFB*, as in the case of *pClFB*, are taken from the gas phase spectrum of Narasimham et al. [34] where possible, with the values for D_{11} and D_{20} obtained from observed hot bands in the electronic spectrum of vapour phase *pBrFB* [37]. The remaining values are taken from the liquid phase IR study of Green [22] with the exception of the value assigned to D_9 which come from the liquid IR spectrum of Patel et al. [36].

There are no gas phase studies of the heavier asymmetric *para*-dihalobenzenes. The values shown in Table 3 for *pFIB* are all taken from Green [22] with the exception of that assigned to D_9 , which is taken from the liquid phase Raman spectrum of Narasimham et al. [34] All values for *pBrClB* are taken from Green [22] except for D_{29} , D_{28} and D_{23} where we include the values tabulated in Ref. 38 which are taken from Paulsen [39] and Herz et al.[24] For *pClIB*, most of the values are taken from Green [22], with the remaining wavenumbers taken from Stojiljković and Whiffen [38], including several values tabulated therein from Ref. [40]. Finally, for *pBrIB*, excluding the value assigned to

D_{28} , which is taken from Stojiljković and Whiffen [38], all wavenumbers are those reported by Green [22].

Occasionally there are vibrations that have not been observed, notably those of a_2 symmetry, and D_{17} for $p\text{BrIB}$ – these have been estimated in Ref. [22], and are given here in parentheses in Table 3.

We note that when moving from the symmetric to the asymmetric dihalobenzenes, the D_5 and D_6 vibrations develop from being in-phase and out-of-phase combinations of the C-X stretch to being localized C-X and C-Y stretches, which are illustrated in Figure 9. For the symmetric cases, the in-phase combination is of the higher wavenumber, while for the asymmetric cases we simply order these in terms of their wavenumber. We note that the D_7 vibration, which does not involve any substantial motion of the substituent atoms, stays at approximately the same value; as a consequence the ordering of the D_i vibrations is not always by wavenumber (see Table 3). Further, we find that across the series, one can identify the C-F stretches at $\sim 1230\text{--}1260\text{ cm}^{-1}$, the C-Cl stretches at $\sim 1080\text{--}1100\text{ cm}^{-1}$, the C-Br stretches at $\sim 1060\text{--}1080\text{ cm}^{-1}$ and the C-I stretches at $\sim 1050\text{--}1070\text{ cm}^{-1}$. In different molecules these stretches may have different D_i labels, but by construction the one involving the lighter halogen will be D_5 and have the highest wavenumber, and that involving the heavier halogen will be D_6 , as a result both of the reduced mass effect and also because of the expected bond strengths. In Figure 9 we show the D_5 and D_6 vibrations for $p\text{FIB}$, where it can be seen that the modes are far more like localized C-X stretches. It is also revealing to note the mixings in terms of the M_i modes in Table 1, where both of the D_5 and D_6 modes have dominant contributions from the M_6 vibration (the C-X stretch in the monohalobenzenes), consistent with their dominant motions.

A similar picture also plays out for the D_{29} and D_{30} vibrations. It may be seen from Figure 4 that for the symmetric $p\text{C}_6\text{H}_4\text{X}_2$ molecules, these consist of in-phase and out-of-phase in-plane bending motion. In D_{30} the motions are in-phase with the two substituent atoms moving one way, while all other atoms move the other way to compensate. In the case of asymmetric substitution, the motion is somewhat different and D_{30} becomes more like a localized in-plane bending mode of the heavier substituent although its form is still recognizable from the mode diagram in Figure 4. With regards to D_{29} , for symmetrically-substituted benzenes (Figure 4), the two substituents are moving out of phase, in opposite directions, so that the other atoms perform a contrarotary motion to compensate. In the asymmetrically-substituted case this motion becomes much more like a localized in-plane bending mode of the lighter atom, but again the form is still recognizable from the mode diagram in Figure 4.

Finally, we note that we might have expected the in-phase and out-of-phase in-plane stretches, D_9 and D_{10} to become more localized versions of each other in the cases of the asymmetric molecules; however, the modes themselves were not so clear on this point, and some semblance of in- and out-of-phase character seems to remain, presumably arising from the substantial motion of other atoms required to keep the centre of mass fixed. The modes can be straightforwardly labelled by their

wavenumber order and also by reference to the relevant mode diagrams in Figure 4. With regard to the out-of-plane “wagging” modes, D_{19} and D_{20} , we see that the former is largely a ring puckering mode, but this motion is a consequence of the out-of-phase, out-of-plane wagging of the two substituents; this ring puckering motion remains in the asymmetrically-substituted molecules, but with a reduced involvement of the heavier atom. The D_{20} mode can be seen to be an in-phase, out-of-plane motion of the two substituents and as such, the ring atoms move out-of-plane to compensate for this; when the substitution becomes asymmetric, the displacement of the heavier atom is reduced, but the other motions are very similar. As such, both D_{19} and D_{20} are straightforwardly identified from the mode diagrams given in Figure 4.

It may be seen from Table 3 that the agreement between the explicitly calculated and experimental values is exceptionally good, and also that the few estimated values from Ref. [22] also concur with the calculated values. Further, in Figure 7, we show the mass trends of the *para*-halofluorobenzenes together with the experimental data. In these cases we have employed the *p*DFB force field and artificially changed the mass of one of the fluorines to match that of the other desired halogen atom. In general there is remarkably good agreement between the two sets of values, with some deviation for the lowest wavenumber vibrations, perhaps partially caused by more severe anharmonic effects in the experimental values than are accounted for by the 0.97 global scaling of the B3LYP/aug-cc-pVTZ calculated values. Additionally, many of these values will not have been adjusted for interactions with overtones and combinations, such as via Fermi resonance. Hence, overall, the isotopic values are sufficient to obtain a reasonable value for any vibration and, further, visualization of the vibrational normal modes confirms the D_i assignments. This is made evident in the Duschinsky matrices given in Figure 8, where largely diagonal behaviour is seen. We have also found that we have not had any difficulty in assigning a D_i label to the vibrations of the other (non-fluoro) asymmetric dihalobenzenes, using this approach, and these data are included in Table 3.

The above comments highlight that we are able to associate a D_i label to both symmetrically and asymmetrically-substituted *p*-dihalobenzenes, where the same label is given to vibrations with the same motion in each molecule. It is then straightforward to compare vibrations across, as well as within, families of molecules – we anticipate this will be important when making deductions based upon vibrational motions, such as in intramolecular vibrational redistribution (IVR) or other vibrationally-induced photophysical phenomena.

From the mass correlation diagram in Figure 7, we can see that there is again generally excellent agreement between the “iso” calculated wavenumbers, indicated by the lines, and the experimental values, indicated by the symbols. The agreement appears to be slightly better than with the symmetrically-substituted species, but as with the symmetric cases discussed above, it appears that the force field changes enough to deviate visibly from the “iso” calculation. It is interesting to note that

for the pairs of vibrations D_9/D_{10} and D_{29}/D_{30} , the lower wavenumber partner deviates further from the “iso” line with increasing mass than the higher wavenumber component, which is localized to the C–F bond and follows the “iso” line closely; this suggests that the local mode nature of these vibrations is largely a result of the mass difference between the halogens, rather than evolving electronic effects arising from the size and electronegativity of the halogen atoms. For the D_{19}/D_{20} pair of vibrations, a slight deviation from the “iso” line occurs with increasing mass for D_{20} , with all experimental wavenumbers lying below the “iso” line for D_{19} , again with a slightly mass dependent deviation between the “iso” and experimental wavenumber observed.

2. *p*-halotoluenes

In Table 4 we include selected experimental data for the *p*-halotoluenes, which we discuss briefly. For *para*-fluorotoluene (*p*FT, with the other molecules abbreviated similarly) we have given the IR results of the liquid phase spectra from Green [22] in the cases where gas-phase values do not exist; however, assignments from gas phase studies are favoured when they are available. We take the values for D_{10} and D_{16} from the high resolution rovibrational studies of Ghosh [41,42]. We also take the values from bands observed in emission following vibronic excitation of *p*FT from coronal discharge from Ha et al. [43]. Although the vibrational fundamental in the latter (Table 3 of that work) appears to be correct, the harmonic wavenumbers and anharmonic constants in their Table 2 must be erroneous (the vibrational spacing is larger than that of the derived harmonic wavenumber). These fundamental values are also consistent with the hot bands observed in the earlier room temperature electronic spectrum of Seliskar et al. [44]. We shall highlight any cases where the selection of the wavenumber value was not straightforward. A value of 1001 cm^{-1} for D_8 is taken from the dispersed fluorescence study of Okuyama et al. [45] which is in excellent agreement with our calculated wavenumber of 1005 cm^{-1} , but lower than the value of 1017 cm^{-1} proposed by Green [22].

The wavenumber of 385 cm^{-1} assigned by Ha et al. [43] to a fundamental we deduce to be D_{14} was obtained from combination bands, and is significantly lower than that assigned to the heavier halotoluenes (*vide infra*); combined with the agreement across the series between the calculated and experimental value, we favour the higher wavenumber value of 404 cm^{-1} assigned to this vibration from the liquid phase IR study of Green [22]. A value of 288 cm^{-1} from Ha et al. [43] may be assigned to the D_{30} vibration, which is in agreement with the value of 287 cm^{-1} determined by Okuyama et al. [45]. However, as Table 4 shows, this value is not in keeping with the trend across the other halotoluenes, nor with the trend for the calculated value to be consistently $10\text{--}15\text{ cm}^{-1}$ too low. For these reasons, we favour the 313 cm^{-1} value from Green [22] for this vibration.

Okuyama et al. [45] cite a wavenumber of 180 cm^{-1} , which we assign to the D_{20} mode, a value that seems substantially too high; however, from currently unpublished work in our group we believe this band is likely to arise from a torsion-vibration level, and this is also likely the case for the

aforementioned 288 cm^{-1} feature. We therefore employ Green's value of 158 cm^{-1} [22] for this vibration, which is more in line with the trend for this mode, and with the calculated value. We also believe that the 1630 cm^{-1} value [45] for D_3 is too high compared to the values for this vibration in the heavier halotoluenes and it does not fit with the trend for the calculated values that are seen to be consistently $\sim 10\text{ cm}^{-1}$ below the experimental values. We therefore favour the value of 1603 cm^{-1} from the liquid phase IR study of Green [22] for this vibration.

The only gas phase studies of *p*CIT in which the vibrations of the S_0 electronic state have been investigated are the dispersed fluorescence experiments of Ichimura et al. [46] and Kojima et al. [47] in which, for all but one case, the observed wavenumbers were in agreement (within an experimental uncertainty of $\sim \pm 5\text{ cm}^{-1}$) with those of the previous liquid phase IR/Raman study of Green [22] with the latter given in Table 4. The exception to this is the 1003 cm^{-1} band observed in the DF spectra of Kojima et al. [47] which we assign to D_8 , in excellent agreement with the calculated wavenumber of this vibration.

There have been no gas phase studies of *p*BrT, with the vibrational wavenumbers determined in the liquid phase IR/Raman spectra of Green [22], being employed in Table 4. Although there is generally excellent agreement with the later study of Balfour and Ristic-Petrovic [48], who recorded liquid-phase Raman and gas-phase electronic spectra, we note that the value for D_{10} (Wilson mode ν_{6a}) was cited as 599 cm^{-1} by Balfour and Ristic-Petrovic, but is in fact noted as being the IR value of Green (which is given as 590 cm^{-1} in that work [22]); since also all of the other values match those of Green [22] exactly, this seems to be a transcription error. (Interestingly, however, a 1-0 hot band is assigned at -601 cm^{-1} in the electronic spectrum of Balfour and Ristic-Petrovic and assigned to this vibration, along with a Raman band observed at 598 cm^{-1} , so there is some ambiguity here.) A 18 cm^{-1} discrepancy between the IR and Raman wavenumbers occurs for D_{23} [22], with the lower wavenumber IR assignment being favoured based on the trends in the calculated wavenumbers throughout the *para*-halotoluene series.

Finally, wavenumbers obtained from the liquid phase IR/Raman study of Green [22] for *p*IT are given in Table 4, with the IR values favoured in the cases when both are available.

Owing to the mass difference, but particularly in the force constants of the C–X and C–CH₃ bonds, rather than the in-phase and out-of-phase C–X stretches, modes D_5 and D_6 of the symmetric dihalobenzene molecules have become localized stretches here (see Figure 9), as was the case for the asymmetric dihalobenzenes. For consistency the C–X stretch is assigned to D_5 and the C–CH₃ stretch is assigned to D_6 . (Note that for the asymmetric dihalobenzenes, a particular C–X stretch could be assigned to either D_5 or D_6 .) For *p*FT, these localized stretches are at a higher wavenumber than D_7 , with the C–CH₃ stretch having a lower wavenumber than the C–F stretch, contrary to expectations based on the masses of the substituents, but rather a testament to the high C–F bond strength.

However, a significant decrease in vibrational wavenumber of D_5 occurs for *p*CIT, with this vibration occurring at a lower wavenumber than both D_6 and D_7 , with further, but smaller, lowering of the wavenumber observed when moving to *p*BrT and *p*IT. It is notable that the vibrational wavenumber of D_7 remains approximately constant throughout the *para*-halotoluene series, in line with its motion not involving the substituent groups lying to lower wavenumber than the C–CH₃ stretch which is seen at ~1205-1215 cm⁻¹.for the halotoluenes.

We also see that the D_{19} and D_{20} vibrations have a similar form to that discussed above for the asymmetric dihalobenzenes, being mainly associated with the C–CH₃ and C–X wags, respectively, although there is still some mixing between these. Finally, the D_{29} and D_{30} vibrations become more localized in-plane bending modes for C–CH₃ and C-X respectively, but again with some mixing.

From the mass correlation diagram in Figure 10, we see generally extremely good agreement between the experimental and “iso” vibrations, but as with the symmetric dihalobenzene cases discussed above, it appears that the force field changes enough from that of *p*DFB to lead to vibrations that deviate visibly from the “iso” calculation for the pairs of vibrations D_9/D_{10} , D_{19}/D_{20} and D_{29}/D_{30} , which assumes these are the same. This is contrary to what was observed for the asymmetrically substituted dihalobenzenes in which the higher wavenumber mode of each pair was a more localized C–F motion, which showed little variation in wavenumber with increasing mass of the second halogen substituent; this can be taken as indicating that although these vibrations are more localized in the halotoluenes than the readily recognizable in-phase and out-of-phase pairs for the symmetrically substituted benzenes, the localization of these modes is not complete, even for *para*-iodotoluene. The wavenumber of D_6 , the C–CH₃ stretch on the other hand remains almost unchanged throughout the halotoluenes, indicating that this mode is essentially uncoupled from its energetic neighbours.

3. phenols

We shall now discuss the assignments of the vibrations of the *p*-halophenols, and then extend the procedure to *p*-cresol. As with the molecules above, we favour gas-phase values where available and then liquid and solid ones. In cases where a vibrational wavenumber has been obtained from both IR and Raman, we favour the IR value for consistency in the selection and not based on any reliability criterion. The selected values are presented in Table 5 and we initially consider the *p*-halophenols.

For the *p*XPhOH series (where X is a halogen), we find trends very similar to those noted above for the asymmetric fluorohalobenzenes and the *p*-halotoluenes. This is not unexpected since the masses of F, CH₃ and OH are very similar. We note that D_5 can be associated with the local C–OH stretching mode, which is almost constant at ~1255–1265 cm⁻¹, while D_6 can be associated with the C–X stretch, which has a value similar to the corresponding vibration in the other molecules, consistent with the mass of X. Similar comments also apply to the D_{29} and D_{30} modes, which become more localized in-

plane bends, and similarly for the the out-of-plane “wagging” modes D_{19} and D_{20} , but still with some mixing in both cases.

For *para*-fluorophenol (*p*FPhOH, with similar abbreviations for the other halophenols) the majority of the values come from dilute solution or liquid phase IR data from Green et al. [49]. A few values were available from the gas-phase dispersed fluorescence study of Biswas et al. [50] which were taken when these values differed from those of previous solution phase work by more than an estimated experimental uncertainty of ± 5 cm^{-1} that we based on the FWHM of the observed bands. An IR dilute solution value for D_{28} from Zierkiewicz et al. [51] was also employed. Notably, the value of 153 cm^{-1} that was assigned to D_{20} , based on the observed overtone in the dispersed fluorescence spectrum of Biswas et al. [50] is in excellent agreement with our calculated wavenumber. This is significantly lower than the 175 cm^{-1} solution/liquid assignment of Green et al. [49] suggesting that this mode is particularly sensitive to solvation/hydrogen bonding. The wavenumber assigned to D_{14} is from the observed overtone in the DF spectrum of Biswas et al. [50]; however, this overtone is perturbed by a Fermi resonance interaction with D_9 , as evinced by the observation of D_9 in the dispersed fluorescence spectrum following excitation to the S_1 $16a^2$ level. Since D_{14}^2 is the dominant contribution to the lower wavenumber eigenstate, the observed wavenumber must be lower than the unperturbed wavenumber; hence the derived fundamental vibrational wavenumber is also expected to be lower than the true value. The only reported observation of this fundamental vibration is the 390 cm^{-1} value of Green et al. [49] from an IR spectrum of a solid sample of *p*FPhOH which is significantly lower than expected for this vibration. We note that an unassigned band at 1201 cm^{-1} is observed in the DF spectrum following excitation of the S_1 vibrationless origin [50] and it is tempting to assign this value to D_6 as it is identical to the calculated wavenumber, however, the calculated values for this mode are typically underestimated compared to the assigned experimental wavenumbers for all other asymmetric *para*-disubstituted benzenes, so we refrain from doing so in this case.

For *p*ClPhOH we preferentially take available gas-phase dispersed fluorescence values from Imhof and Kleinermanns [52] but the majority are taken from the dilute solution values from Green et al. [49] with two values taken from the solution spectra of Zierkiewicz et al. [53]. These assignments are straightforward, although it is worth noting that Green et al. [49] report a value of 160 cm^{-1} for the vibration which we denote as D_{20} , while Imhof and Kleinermanns [52] report 123 cm^{-1} , with the latter being in excellent agreement with the present calculated value. We then note that Green et al. [49] did observe a band at 122 cm^{-1} , but have assigned to a hydrogen-bond vibration – it seems likely the Imhof and Kleinermanns [52] assignment is correct. Also we note that a value of 1023 cm^{-1} was reported for an a_1 fundamental in Ref. [52], but the value of Green et al. [49] agrees better with our calculated value. The fundamental wavenumber for D_{14} is derived from the observed overtone in the DF spectrum of Imhof and Kleinermanns [52], which as in the case of *p*FPhOH appears to be in Fermi

resonance with D_9 , and so similar comments regarding this derived fundamental wavenumber made in that case apply here.

For *p*BrPhOH, almost all of the values are from the dilute solution IR spectrum of Green et al. [49], with three values coming from Zierkiewicz et al. [53]. Again we note that Green et al.'s value [49] for the vibration we denote as D_{20} of 151 cm^{-1} is not in good agreement with the calculated value, but again a low wavenumber band (assigned to hydrogen bonding therein) at 103 cm^{-1} is in very good agreement. For *p*IPhOH the only values available seem to be the IR values from Green et al. [49] so there are a number of unassigned vibrations here. Interestingly, again the suggested value for D_{20} from that work is significantly higher than the present calculated value, but again a low wavenumber band at 97 cm^{-1} is in excellent agreement with the calculated value, but had been assigned to hydrogen bonding. We have entered these low-wavenumber bands as D_{20} in Table 5.

The values in Table 5 for *p*-cresol predominantly come from the gas-phase IR results of Arp et al. [54] with one value coming from the gas phase IR spectrum of Jakobsen [55] while in the cases where values were not available, the liquid-phase IR and then Raman values were employed, with the preference in that order from the same work; a couple of the values are taken from the liquid phase Raman spectrum of Jakobsen [55]. From the IR spectrum of a dilute solution of *p*-cresol, Green et al. [49] assigns a value of 178 cm^{-1} to a fundamental vibration which corresponds to D_{20} , which is significantly higher than the 161 cm^{-1} value reported by Jakobsen [55] with both values higher than the calculated value of 141 cm^{-1} [55]. As in the cases of the heavier halophenols, Green et al. [49] observe a low wavenumber band assigned to hydrogen bonding; however, for *p*-cresol, the assigned value of 125 cm^{-1} is lower than expected for this vibration, and therefore an unlikely assignment for D_{20} .

Inspection of the mass correlation diagram in Figure 11 leads to similar conclusions to be drawn as for the *para*-halotoluenes, with generally very good agreement between the experimental and "iso" vibrations. Again it appears that the force field changes enough from that of *p*DFB that the calculated vibrational wavenumbers deviate visibly from the "iso" calculation, for the pairs of vibrations D_9/D_{10} , D_{19}/D_{20} and D_{29}/D_{30} . The mode with the more localized C–OH character, assigned to D_5 , lies above the C–X stretch for all halophenols, in line with the expected wavenumber ordering based on mass of the substituents, contrary to what was observed for the halotoluenes. For *p*FT, the mode with more localized C–F stretching character (D_5) has a higher wavenumber than the C–CH₃ mode (D_6). This may be rationalized by the smaller mass difference between OH and F, than between the CH₃ group and F, combined with the stronger C–OH bond as evinced by the higher calculated wavenumber for D_5 [C–OH] in FPhOH of 1244 cm^{-1} , compared to that of D_6 [C–CH₃] in *p*FT of 1215 cm^{-1} , despite the higher mass of OH.

V. CONCLUSIONS

In this paper we have examined the vibrational modes of a range of *para*-disubstituted benzenes, including both symmetric and asymmetric species. To allow a single labelling scheme we based it on the C_{2v} point group and were able to show that the labels can be applied across a range of different molecules. Even in the cases of halophenols and halotoluenes, the method works well. It is therefore possible to compare corresponding vibrations across species, and hence be sure that one is comparing “like for like” when photophysical behaviour is being assessed between molecules. The only aspect where caution was required was with respect to the D_5 and D_6 , and D_{29} and D_{30} pairs of vibrations, which are in- and out-of-phase versions of each other in symmetrically-substituted molecules, but become localized modes in asymmetrically-substituted molecules, particularly when the mass difference between the substituents is great. Assignment of the vibrations can be made by calculating artificial isotope (“iso”) vibrational wavenumbers, and comparing the normal modes with those presented in Figure 4 (and also Figure 9, for selected asymmetric cases).

We have discussed the evolution of the Wilson vibrational modes of benzene into those of *p*DFB, and have also examined the intermediate step with FBz. We conclude from these examinations that one cannot always simply look at a mode in isolation and deduce how it will change as one or more of the substituent’s mass changes, but rather one may have to consider pairs (or more) of vibrations and see how these combine as a result of the substitution. In this way, we gained some insight into why it was that some vibrations appeared to have little dependence on mass variation, while others were strongly dependent. In addition, we were able to trace contributions of vibrations through “avoided crossings”: some vibrations passed through these avoided crossings essentially maintaining their character (in terms of Wilson or M_i modes), while others became very mixed as a result of several such crossings. The result was that *some* vibrations could still be described by Wilson-type labels, but *many could not*. Indeed, many were so mixed that no single Wilson label could come close to being associated with those vibrations.

In summary, as with our labelling scheme for monosubstituted benzenes [2] we anticipate that use of the present D_i scheme will bring consistency to the labelling of such modes and hopefully become widely used by the community.

ACKNOWLEDGEMENTS.

We are grateful to the EPSRC for funding via grant EP/L021366/1. The EPSRC and the University of Nottingham are thanked for studentships to A.A. and W.D.T. We are grateful to the NSCCS for the provision of computer time under the auspices of the EPSRC, and to the High Performance Computer

resource at the University of Nottingham. Alison J. Lee, Andrew Claydon, Joe Carter, Angus Taylor, Jodie McDaniel are thanked for preliminary work as part of undergraduate research projects.

Table 1. Labelling schemes for the S_0 vibrations of p DFB and Varsányi's p DCIB

Mode ^a	Mixed (Bz) ^b	Mixed (FBz) ^c	p DFB - Varsányi ^d	p DCIB - Varsányi ^d
a_1				
$D_1(a_g)$	2,7a	$M_1,(M_3)$	20a	2
$D_2(b_{1u})$	13,20a	$M_3,M_2,(M_1)$	2	13
$D_3(a_g)$	9a	M_4	8a	8a
$D_4(b_{1u})$	18a,(20a)	M_5	19a	19a
$D_5(a_g)$	1,7a,(2,6a)	$M_6,M_9,(M_2,M_3,M_8)$	7a	1
$D_6(b_{1u})$	12,19a,20a,(13 18a)	$M_6,M_9,(M_2,M_3)$	13	12
$D_7(a_g)$	8a	M_7	9a	9a
$D_8(b_{1u})$	19a,12	$M_8,(M_9)$	18a	18a
$D_9(a_g)$	1,6a,(7a,2)	$M_{10},(M_9,M_2)$	1	6a
$D_{10}(b_{1u})$	20a,12,(19a,13)	$M_{10},(M_{11},M_9,M_2,M_3)$	12	20a
$D_{11}(a_g)$	6a,7a,(2,1)	$M_{11},(M_2,M_3)$	6a	7a
a_2				
$D_{12}(a_u)$	17a	M_{12}	17a	17a
$D_{13}(b_{1g})$	10a	M_{13}	10a	[10a]
$D_{14}(a_u)$	16a	M_{14}	[16a]	16a
b_1				
$D_{15}(b_{2g})$	5,10b	M_{15},M_{16}	5	5
$D_{16}(b_{3u})$	17b,11,(16b)	$M_{16},M_{17},(M_{15},M_{18})$	17b	17b
$D_{17}(b_{2g})$	4,(10b)	M_{18},M_{17}	4	4
$D_{18}(b_{3u})$	16b,11,(17b)	$M_{19},(M_{18},M_{17})$	16b	16b
$D_{19}(b_{2g})$	10b,4,(5)	$M_{20},(M_{19},M_{18},M_{17},M_{15})$	10b	10b
$D_{20}(b_{3u})$	16b,17b,11	$M_{20},(M_{17},M_{15},M_{16},M_{18})$	11	[11]
b_2				
$D_{21}(b_{2u})$	20b	M_{21},M_{22}	7b	20b
$D_{22}(b_{3g})$	7b	M_{22},M_{21}	20b	7b
$D_{23}(b_{3g})$	9b	M_{23}	[8b]	[8b]
$D_{24}(b_{2u})$	18b,(19b,14,15)	$M_{24},(M_{25},M_{27})$	19b	19b
$D_{25}(b_{2u})$	15,(14)	$M_{26},M_{25},(M_{27})$	14	14
$D_{26}(b_{3g})$	3,8b	$M_{26},M_{25},(M_{27})$	3	3
$D_{27}(b_{2u})$	14,19b	M_{28},M_{27}	18b	18b
$D_{28}(b_{3g})$	6b,(8b)	$M_{29},(M_{27})$	6b	6b
$D_{29}(b_{3g})$	8b,6b,(3)	$M_{30},(M_{27},M_{29},M_{28})$	9b	9b
$D_{30}(b_{2u})$	19b,14,18b	$M_{30},(M_{27},M_{28},M_{24})$	15	15

^aNumbered according to the Mulliken convention in C_{2v} symmetry (see text), with the label in parentheses corresponding to the symmetry of the vibration within the D_{2h} point group.

^b Normal modes of p DFB expressed in terms of those of Bz using a generalized Duschinsky approach – see text.

^c Normal modes of p DFB expressed in terms of those of FBz using a generalized Duschinsky approach – see text.

^d From Ref. 5 – we have made our best attempt at determining the correspondences based on the wavenumbers cited in that work, and those we present in Table 2.

Table 2: Vibrational wavenumbers for $p\text{-C}_6\text{H}_4\text{X}_2$ (X = F, Cl, Br, I, CH₃ and OH)^a

Mode			$p\text{Xyl}$		HQ		$p\text{DFB}$		$p\text{DCIB}$		$p\text{DBrB}$		$p\text{DIB}$	
D_i	D_{2h}^b	C_{2h}^c	Experimental	Calculated ^d	Experimental	Calculated ^d	Experimental	Calculated ^d						
a_1														
D_1	$1(a_g)$	$1(a_g)$	3059 ^e	3073	3070 ^f	3100	3088 ^g	3114	3070 ^h	3114	3068 ⁱ	3113	3056 ⁱ	3109
D_2	$10(b_{1u})$	$21(b_u)$	3045 ^e	3054	3037 ^j	3061	3073 ^g	3100	3098 ^k	3100	3068 ^l	3098	3055 ⁱ	3094
D_3	$2(a_g)$	$2(a_g)$	1616 ^e	1606	1618 ^f	1614	1615 ^g	1595	1574 ^h	1563	1570 ⁱ	1551	1552 ⁱ	1540
D_4	$11(b_{1u})$	$22(b_u)$	1520 ^e	1505	1521 ^m	1502	1514 ^g	1492	1478 ^k	1463	1468 ^l	1458	1463 ⁱ	1455
D_5	$3(a_g)$	$3(a_g)$	1203 ^e	1186	1262 ^f	1245	1257 ^g	1226	1096 ^h	1067	1067 ⁱ	1045	1044 ⁱ	1031
D_6	$12(b_{1u})$	$23(b_u)$	1225 ^e	1203	1249 ^m	1226	1228 ^g	1187	1094 ^k	1067	1078 ^l	1056	1069 ⁱ	1055
D_7	$4(a_g)$	$4(a_g)$	1183 ^e	1173	1162 ^f	1148	1140 ^g	1126	1169 ^h	1160	1170 ⁱ	1166	1175 ⁱ	1173
D_8	$13(b_{1u})$	$24(b_u)$	1026 ^e	1011	1005 ^j	997	1014 ^g	999	1017 ^k	1000	1003 ^l	991	993 ⁱ	982
D_9	$5(a_g)$	$5(a_g)$	830 ^e	813	854 ^f	838	859 ^g	841	747 ^h	730	708 ⁱ	699	680 ⁱ	680
D_{10}	$14(b_{1u})$	$25(b_u)$	694 ^e	712	754 ^m	742	740 ^g	724	545 ^k	523	424 ^l	410	361 ⁱ	356
D_{11}	$6(a_g)$	$6(a_g)$	454 ^e	449	468 ^f	458	450 ^g	443	328 ^h	318	218 ⁱ	205	157 ⁱ	153
a_2														
D_{12}	$7(a_u)$	$12(a_u)$	972 ^e	961	937 ⁿ	926	945 ^g	939	951 ^h	954	950 ^l	956	951 ⁱ	959
D_{13}	$9(b_{1g})$	$17(b_g)$	832 ^e	830	806 ^f	786	800 ^g	792	815 ^h	809	815 ^l	810	816 ⁱ	814
D_{14}	$8(a_u)$	$13(a_u)$	410 ^e	408	410 ⁿ	418	422 ^o	424	410 ^h	406	402 ^l	402	(400) ⁱ	397
b_1														
D_{15}	$15(b_{2g})$	$18(b_g)$	930 ^e	935	920 ⁿ	912	928 ^g	927	934 ^h	941	935 ^l	940	936 ⁱ	942
D_{16}	$28(b_{3u})$	$14(a_u)$	795 ^e	792	821 ^m	820	838 ^g	835	819 ^k	821	807 ^l	812	799 ⁱ	803
D_{17}	$16(b_{2g})$	$19(b_g)$	700 ^e	701	703 ^f	705	692 ^g	694	687 ^h	692	(680) ^l	685	(685) ⁱ	676
D_{18}	$29(b_{3u})$	$15(a_u)$	481 ^e	484	513 ^f	507	505 ^g	505	480 ^k	483	473 ^l	473	464 ⁱ	465
D_{19}	$17(b_{2g})$	$20(b_g)$	312 ^e	300	363 ^f	356	374 ^g	363	298 ^h	288	282 ^l	258	241 ⁱ	233
D_{20}	$30(b_{3u})$	$16(a_u)$	132 ^e	132	193 ^j	149	158 ^g	154	125 ^h	99	103 ^l	74		59
b_2														
D_{21}	$18(b_{2u})$	$26(b_u)$	3056 ^e	3070	3023 ^j	3099	3091 ^g	3113	3098 ^k	3113	3078 ^l	3111	(3050) ⁱ	3107
D_{22}	$23(b_{3g})$	$7(a_g)$	3042 ^e	3054		3063	3085 ^g	3102	3065 ^h	3102	3068 ^l	3099	3056 ⁱ	3095
D_{23}	$24(b_{3g})$	$8(a_g)$	1578 ^e	1564	1604 ^f	1595	1617 ^g	1601	1574 ^h	1563	1565 ^l	1557	1552 ⁱ	1545

Mode			$pXyl$		HQ		$pDFB$		$pDCIB$		$pDBrB$		$pDIB$	
D_{24}	19(b_{2u})	27(b_u)	1400 ^e	1395	1455 ^m	1443	1437 ⁱ	1400	1393 ^k	1378	1381 ^l	1370	1374 ⁱ	1363
D_{25}	20(b_{2u})	28(b_u)	1320 ^e	1281	1332 ^m	1315	1306 ^g	1287	1260 ⁱ	1264	1251 ⁱ	1260	1242 ⁱ	1252
D_{26}	25(b_{3g})	9(a_g)	1313 ^e	1306	1350 ^p	1325	1285 ^g	1268	1290 ^h	1282	1290 ^q	1285	1292 ⁱ	1289
D_{27}	21(b_{2u})	29(b_u)	1099 ^e	1107	1087 ^m	1082	1085 ^g	1074	1112 ^k	1090	1100 ^l	1091	1100 ⁱ	1092
D_{28}	26(b_{3g})	10(a_g)	643 ^e	640	648 ^m	640	635 ^g	628	626 ^h	621	623 ⁱ	618	624 ⁱ	617
D_{29}	27(b_{3g})	11(a_g)	389 ^e	374		436	446 ^o	435	350 ^h	343	307 ^l	301	(255) ⁱ	271
D_{30}	22(b_{2u})	30(b_u)	285 ^e	277	322 ^p	331	348 ^g	337	225 ^k	213	171 ^l	158	140 ^f	126

^a Values in parentheses have been estimated in the cited work.

^b Numbered according to the Mulliken convention in the D_{2h} point group with the symmetry given in parentheses. For D_{2h} the order of the symmetry groups used in assigning the numbering comes from Table 14 in Herzberg II [10] and has the order $A_g, A_u, B_{1g}, B_{1u}, B_{2g}, B_{2u}, B_{3g}, B_{3u}$; the symmetry breakdown of the thirty vibration is $6A_g+2A_u+1B_{1g}+5B_{1u}+3B_{2g}+5B_{2u}+5B_{3g}+3B_{3u}$.

^c Labelled according to the Mulliken convention in the C_{2h} point group with the symmetry given in parentheses, where the order of the symmetry groups used in assigning the numbering comes from Table 13 in Herzberg II [10], and is A_g, A_u, B_g, B_u ; the symmetry breakdown of the thirty vibration is $11A_g+5A_u+4B_g+10B_u$.

^d This work: B3LYP/aVTZ scaled by 0.97.

^e Vapour phase IR and Raman from Ref. [26].

^f Solution phase IR/Raman From Ref. [33].

^g Vapour phase IR from Ref. [15].

^h From Ref. [21].

ⁱ From Ref. [23].

^j From Ref. [32].

Vapour Phase IR from Ref. [20].

^l Liquid IR/Raman from Ref. [22].

^m Vapour phase from Ref. [30].

ⁿ Nujol mull IR from Ref. [28].

^o Dispersed fluorescence from Ref. [19].

^p Nujol mull of the solid from Ref. [29].

^q From Ref. [24].

^r Solution phase IR from Ref. [25].

Table 3: Vibrational wavenumbers for $p\text{-C}_6\text{H}_4\text{XY}$: asymmetric *para*-dihalobenzenes^a

Mode	$p\text{ClFB}$		$p\text{BrFB}$		$p\text{FIB}$		$p\text{BrClB}$		$p\text{ClIB}$		$p\text{IBrB}$	
	Experimental	Calculated ^b	Experimental	Calculated ^b	Experimental	Calculated ^b	Experimental	Calculated ^b	Experimental	Calculated ^b	Experimental	Calculated ^b
a_1												
D_1	3076 ^c	3114	3076 ^c	3113	3072 ^c	3111	3070 ^c	3113	3067 ^c	3111	3069 ^c	3111
D_2	3076 ^c	3099	3076 ^c	3099	3072 ^c	3097	3070 ^c	3099	3052 ^d	3097	3069 ^c	3096
D_3	1592 ^c	1581	1587 ^c	1576	1589 ^c	1572	1570 ^c	1557	1567 ^c	1552	1553 ^c	1546
D_4	1490 ^c	1477	1485 ^c	1474	1484 ^c	1471	1471 ^c	1461	1470 ^c	1459	1467 ^c	1457
D_5	1233 ^{c (C-F)}	1211 ^(C-F)	1236 ^(C-F)	1211 ^(C-F)	1230 ^(C-F)	1211 ^(C-F)	1087 ^(C-Cl)	1067 ^(C-Cl)	1090 ^{c (C-Cl)}	1068 ^(C-Cl)	1069 ^{c (C-Br)}	1057 ^(C-Br)
D_6	1096 ^(C-Cl)	1064 ^(C-Cl)	1069 ^(C-Br)	1046 ^(C-Br)	1050 ^(C-I)	1037 ^(C-I)	1068 ^(C-Br)	1051 ^(C-Br)	1054 ^{c (C-Br)}	1042 ^(C-Br)	1052 ^{c (C-I)}	1038 ^(C-I)
D_7	1153 ^c	1141	1157 ^c	1144	1158 ^c	1147	1166 ^c	1163	1172 ^c	1167	1171 ^c	1170
D_8	1017 ^c	1002	1015 ^c	1000	1011 ^c	998	1009 ^c	996	1005 ^c	992	1000 ^c	987
D_9	815 ^f	809	812 ^f	805	806 ^g	802	730 ^c	716	722 ^c	709	697 ^c	690
D_{10}	639 ^e	616	600 ^e	580	575 ^c	565	496 ^c	477	476 ^c	460	397 ^c	386
D_{11}	375 ^c	364	282 ^h	278	244 ^c	236	258 ^c	251	220 ^c	214	180 ^c	177
a_2												
D_{12}	949 ^c	948	945 ^c	949	949 ^c	951	951 ^c	955	951 ^c	957	954 ^c	957
D_{13}	805 ^c	800	804 ^c	800	800 ^c	801	812 ^c	809	(815) ^c	811	(813) ^c	812
D_{14}	(405) ^c	416	(405) ^c	414	(405) ^c	411	405 ^c	404	400 ^c	402	(400) ^c	400
b_1												
D_{15}	936 ^c	935	931 ^c	934	931 ^c	935	935 ^c	941	936 ^c	942	936 ^c	941
D_{16}	830 ^e	829	827 ^e	826	821 ^c	823	812 ^c	817	809 ^c	813	803 ^c	808
D_{17}	690 ^c	693	689 ^c	690	688 ^c	685	686 ^c	689	686 ^c	685	(685) ^c	681
D_{18}	498 ^c	497	496 ^c	495	497 ^c	493	480 ^c	479	476 ^c	475	470 ^c	469
D_{19}	337 ^e	326	322 ^e	312	309 ^c	300	291 ^c	273	275 ^c	261	261 ^c	246
D_{20}	130 ^c	123	127 ^h	108	112 ^c	98	112 ^c	86	103 ^c	78	97 ^c	66
b_2												
D_{21}	3076 ^c	3112	3076 ^c	3112	3072 ^c	3110	3082 ^c	3112	3073 ^c	3110	3089 ^c	3109
D_{22}	3076 ^c	3101	3046 ^c	3101	3072 ^c	3099	3082 ^c	3100	3073 ^c	3098	3089 ^c	3097
D_{23}	1592 ^c	1583	1587 ^c	1581	1579 ^c	1577	1557 ⁱ	1559	1560 ^k	1554	1553 ^c	1551
D_{24}	1402 ^c	1389	1400 ^c	1384	1393 ^c	1380	1390 ^c	1374	1387 ^c	1370	1374 ^c	1366
D_{26}	1266 ^c	1278	1277 ^c	1279	1260 ^c	1282	1216 ^c	1283	1215 ^c	1286	1213 ^c	1287
D_{25}	1287 ^c	1274	1290 ^c	1273	1293 ^c	1268	1290 ^c	1262	1289 ^c	1257	1296 ^c	1256
D_{27}	(1086) ^j	1082	1086 ^c	1082	1086 ^c	1082	1100 ^c	1091	1100 ^c	1092	1100 ^c	1092
D_{28}	630 ^c	624	624 ^c	622	626 ^c	620	624 ^l	619	624 ^k	618	623 ^k	617
D_{29}	419 ^c	412	416 ^c	407	413 ^c	405	333 ^l	326	324 ^d	317	294 ^c	288
D_{30}	265 ^c	254	218 ^e	212	196 ^c	185	194 ^c	182	173 ^c	161	155 ^c	141

^a Values in parentheses have been estimated in the cited work. Where the same wavenumber value is given for two vibrations of the same symmetry group, the assignment is assumed to be uncertain. The pairs of modes, D_5/D_6 and D_{29}/D_{30} become more localized modes here, while they were in- and out-of-phase combinations for the symmetric cases. The higher value corresponds to a C–X stretch involving the lighter atom, while the lower value corresponds to the corresponding mode involving the heavier atom as indicated – see text.

^b This work: B3LYP/aVTZ scaled by 0.97.

^c IR values from Ref. [22].

^dLiquid phase Raman values from Ref. [40] as tabulated in Ref. [38].

^eVapour phase IR from Ref. [34].

^fLiquid phase IR/Raman from Ref. [36].

^gLiquid phase Raman values from Ref. [34].

^hFrom hot bands observed in vapour phase electronic spectrum from Ref. [37].

ⁱLiquid phase Raman values from Refs. 24 and 39 as tabulated in Ref. [38].

^jEstimate, this work.

^kSolution phase Raman from Ref. [38].

Table 4: Vibrational wavenumbers for *para*-halotoluenes^a

Mode	<i>p</i> FT		<i>p</i> CIT		<i>p</i> BrT		<i>p</i> IT	
	Experimental	Calculated ^b						
<i>a</i> ₁								
<i>D</i> ₁	3068 ^c	3103	3062 ^d	3104	3061 ^c	3104	3058 ^c	3101
<i>D</i> ₂	3068 ^c	3071	3062 ^d	3070	3061 ^c	3069	3058 ^c	3067
<i>D</i> ₃	1603 ^c	1598	1597 ^c	1587	1592 ^c	1582	1587 ^c	1579
<i>D</i> ₄	1513 ^c	1499	1492 ^c	1481	1488 ^c	1477	1486 ^c	1474
<i>D</i> ₅	1241 ^{e (C-F)}	1209 ^(C-F)	1090 ^{c (C-Cl)}	1069 ^(C-Cl)	1069 ^{c (C-Br)}	1054 ^(C-Br)	1059 ^{c (C-I)}	1048 ^(C-I)
<i>D</i> ₆	1215 ^{e (C-Me)}	1192 ^(C-Me)	1209 ^{c (C-Me)}	1193 ^(C-Me)	1212 ^{c (C-Me)}	1192 ^(C-Me)	1209 ^{c (C-Me)}	1192 ^(C-Me)
<i>D</i> ₇	1157 ^c	1145	1176 ^c	1167	1179 ^c	1169	1182 ^c	1173
<i>D</i> ₈	1001 ^f	1005	1003 ^g	1005	1013 ^c	1000	1009 ^c	996
<i>D</i> ₉	843 ^e	827	797 ^d	786	793 ^c	781	787 ^c	778
<i>D</i> ₁₀	730 ^h	715	638 ^c	614	590 ^c	579	575 ^c	566
<i>D</i> ₁₁	453 ^e	446	379 ^c	367	292 ^c	279	245 ^c	238
<i>a</i> ₂								
<i>D</i> ₁₂	956 ^c	953	955 ^c	959	956 ^c	960	948 ^c	961
<i>D</i> ₁₃	810 ^c	808	819 ^d	819	815 ^d	819	810 ^d	822
<i>D</i> ₁₄	404 ^c	418	405 ^c	409	405 ^c	406	404 ^c	403
<i>b</i> ₁								
<i>D</i> ₁₅	929 ^c	931	934 ^c	939	935 ^c	939	936 ^c	940
<i>D</i> ₁₆	819 ⁱ	817	806 ^c	807	801 ^c	802	796 ^c	798
<i>D</i> ₁₇	695 ^c	698	692 ^c	697	692 ^c	695	680 ^c	694
<i>D</i> ₁₈	502 ^c	500	484 ^c	484	476 ^c	478	473 ^c	475
<i>D</i> ₁₉	321 ^e	330	304 ^c	295	292 ^c	284	285 ^c	271
<i>D</i> ₂₀	158 ^c	141	132 ^c	115	121 ^c	102	115 ^c	93
<i>b</i> ₂								
<i>D</i> ₂₁	3040 ^c	3102	3039 ^c	3103	3038 ^c	3103	3037 ^c	3099
<i>D</i> ₂₂	3040 ^c	3071	3027 ^d	3069	3026 ^c	3068	3024 ^c	3067
<i>D</i> ₂₃	1592 ^c	1586	1577 ^c	1565	1570 ^d	1562	1570 ^c	1556
<i>D</i> ₂₄	1435 ^c	1395	1402 ^c	1388	1397 ^c	1384	1393 ^c	1384
<i>D</i> ₂₅	1300 ^c	1283	1279 ^c	1273	1270 ^c	1271	1265 ^c	1266
<i>D</i> ₂₆	1321 ^c	1292	1304 ^c	1295	1299 ^c	1295	1301 ^c	1297
<i>D</i> ₂₇	1099 ^c	1090	1112 ^c	1100	1112 ^c	1101	1111 ^c	1102
<i>D</i> ₂₈	640 ^e	633	634 ^c	631	633 ^c	628	633 ^c	628
<i>D</i> ₂₉	426 ^c	414	374 ^c	363	364 ^c	354	358 ^c	349
<i>D</i> ₃₀	313 ^c	298	254 ^c	241	216 ^c	204	190 ^c	180

^a Values in parentheses have been estimated in the cited work. Where the same wavenumber value is given for two vibrations of the same symmetry group, the assignment is assumed to be uncertain. The pairs of modes, *D*₅/*D*₆ and *D*₂₉/*D*₃₀ become more localized modes here, while they were in- and out-of-phase combinations for the symmetric cases. *D*₅ corresponds to the C–X stretch, while *D*₆ corresponds to the C–Me (i.e. C–CH₃) stretch, as indicated – see text.

^b This work: B3LYP/aVTZ scaled by 0.97.

^cLiquid phase IR from Ref. [22].

^dLiquid phase Raman from Ref. [22].

^eElectronic emission spectrum from Ref. [43].

^fDispersed fluorescence spectra from Ref. [45].

^gDispersed fluorescence from Ref. [47].

^hRotationally resolved gas phase IR from Ref. [41].

ⁱRotationally resolved gas phase IR from Ref. [42].

Table 5: Vibrational wavenumbers for *para*-halophenols ^a

Mode	<i>p</i> -cresol		<i>p</i> FPPhOH		<i>p</i> ClPhOH		<i>p</i> BrPhOH		<i>p</i> IPhOH	
	Experimental	Calculated ^b								
<i>a</i> ₁										
<i>D</i> ₁	3061 ^c	3095	3077 ^d	3108	3064 ^d	3110	3062 ^d	3109	3060 ^d	3106
<i>D</i> ₂	3061 ^c	3054	3050 ^d	3095	3034 ^d	3095	3030 ^d	3094	3025 ^d	3092
<i>D</i> ₃	1612 ^c	1606	1611 ^d	1605	1610 ^d	1591	1588 ^d	1588	1582 ^d	1584
<i>D</i> ₄	1516 ^c	1503	1512 ^d	1497	1494 ^d	1481	1498 ^d	1477	1486 ^d	1474
<i>D</i> ₅	1258 ^{c(C-OH)}	1240 ^(C-OH)	1264 ^{d(C-OH)}	1244 ^(C-OH)	1258 ^{d(C-OH)}	1244 ^(C-OH)	1257 ^{d(C-OH)}	1243 ^(C-OH)	1258 ^{d(C-OH)}	1244 ^(C-OH)
<i>D</i> ₆	1215 ^{c(C-Me)}	1195 ^(C-Me)	1223 ^{d(C-F)}	1201 ^(C-Cl)	1097 ^{e(C-Cl)}	1068 ^(C-Cl)	1068 ^{d(C-Br)}	1051 ^(C-Br)	1053 ^{d(C-I)}	1043 ^(C-I)
<i>D</i> ₇	1172 ^c	1161	1152 ^d	1136	1163 ^d	1155	1164 ^d	1158	1168 ^d	1162
<i>D</i> ₈	1010 ^c	1004	1012 ^d	998	1010 ^d	998	1010 ^d	995	1007 ^d	992
<i>D</i> ₉	840 ^e	828	857 ^f	839	829 ^e	812	810 ^d	808	810 ^d	806
<i>D</i> ₁₀	738 ^c	724	747 ^d	734	646 ^e	625	607 ^d	590	585 ^d	576
<i>D</i> ₁₁	459 ^c	453	457 ^f	450	377 ^e	368	295 ^d	280	246 ^d	238
<i>a</i> ₂										
<i>D</i> ₁₂	953 ^c	952	942 ^d	937	945 ^d	946	945 ^d	947	945 ^d	949
<i>D</i> ₁₃	823 ^h	798	794 ^f	787	801 ^d	793	788 ⁱ	793	(800) ^d	793
<i>D</i> ₁₄	416 ^c	412	418 ^f	421	407 ^e	412	401 ^d	410	(400) ^d	407
<i>b</i> ₁										
<i>D</i> ₁₅	918 ^c	921	918 ^d	916	924 ^d	924	926 ^d	924	925 ^d	925
<i>D</i> ₁₆	819 ^c	819	829 ^d	829	824 ^d	825	821 ^d	823	820 ^d	821
<i>D</i> ₁₇	699 ^c	704	700 ^d	700	696 ^d	696	694 ^d	693	693 ^d	689
<i>D</i> ₁₈	504 ^c	504	507 ^d	506	502 ^d	500	500 ^d	498	497 ^d	497
<i>D</i> ₁₉	294 ^g	321	374 ^d	358	318 ^e	316	319 ^d	303	307 ^d	290
<i>D</i> ₂₀	[161] ^h	141	153 ^f	151	123 ^e	122	103 ^{d*}	108	97 ^{d*}	97
<i>b</i> ₂										
<i>D</i> ₂₁	3029 ^c	3073	3050 ^d	3105	3073 ⁱ	3106	3012 ⁱ	3105		3102

D_{22}	3016 ^c	3054	3036 ^d	3065	3010 ⁱ	3065	3000 ⁱ	3064		3063
D_{23}	1600 ^h	1584	1605 ^d	1596	1592 ^d	1580	1588 ^d	1576	1582 ^d	1572
D_{24}	1428 ^c	1415	1438 ^d	1427	1426 ^d	1415	1430 ^d	1411	1418 ^d	1407
D_{25}	1298 ^c	1293	1323 ^d	1315	1318 ^d	1313	1321 ^d	1312	1318 ^d	1312
D_{26}	1334 ^c	1322	1302 ^d	1281	1284 ^d	1278	1281 ^d	1278	1277 ^d	1275
D_{27}	1114 ^c	1097	1089 ^d	1079	1109 ^d	1088	1092 ^d	1088	1088 ^d	1089
D_{28}	644 ^e	639	640 ^j	634	629 ^d	629	632 ^d	627	(630) ^d	626
D_{29}	416 ^c	415	445 ^d	435	420 ^e	412	418 ^d	408	413 ^d	405
D_{30}	328 ^c	296	348 ^d	334	256 ^e	252	233 ^d	210	208 ^d	185

^a Values in parentheses have been estimated in the cited work. Where the same wavenumber value is given for two vibrations of the same symmetry group, the assignment is assumed to be uncertain. The pairs of modes, D_5/D_6 and D_{29}/D_{30} become more localized modes here, while they were in- and out-of-phase combinations for the symmetric cases. D_5 corresponds to a C–OH stretch, while D_6 corresponds to the corresponding C–X mode, as indicated – see text. D_{10} is perturbed *via* a Fermi resonance interaction with D_{14}^2 —see text.

^b This work: B3LYP/aVTZ scaled by 0.97.

^c Vapour phase IR from Ref. [54].

^d Solution phase IR spectra from Ref. [49].

^e Dispersed fluorescence from Ref. [52].

^f Dispersed fluorescence from Ref. [50].

^g Vapour phase IR from Ref. [55].

^h Liquid phase Raman from Ref. [55].

ⁱ Solution phase IR from Ref. [53].

^j Solution phase IR from Ref. [51].

Figure Captions:

Figure 1: Mass-correlated vibrational wavenumbers showing how the vibrations of Bz evolve into those of *p*DFB. The force field of Bz is employed and the masses of the *ipso* and *para* hydrogen atoms are artificially varied from 1 to 19 amu. The vibrations have been grouped into their C_{2v} symmetry groups: a_1 , a_2 , b_1 and b_2 . The Wilson labels have been included on the left, while on the right hand side the numbers refer to the D_i modes.

Figure 2: Generalized Duschinsky matrix showing how the vibrational modes of *p*DFB can be expressed in terms of the Bz ones – clearly significant mixing of the Bz modes occurs, see text for further discussion. Black shading indicates a normalized coefficient value of 1.00, while white indicates a value of 0.00, with grey shading indicating intermediate values, see text for details.

Figure 3: Mass-correlated vibrational wavenumbers showing how the vibrations of FBz (centre) evolve into those of Bz (left) and to those of *p*DFB (right). Lines and symbols refer to “iso” calculations where the force field for FBz is employed and the mass of the fluorine atom is artificially varied from 19 to 1 amu when moving to the left (where it will mimic Bz), and then that of the *para* hydrogen is varied from 1 to 19 amu when moving to the right (where it will mimic *p*DFB). The vibrations have been grouped into their C_{2v} symmetry groups: a_1 , a_2 , b_1 and b_2 . The Wilson labels have been included on the left; in the centre the numbers refer to the M_i modes, while on the right hand side, the numbers refer to the D_i modes.

Figure 4: Calculated vibrational modes for *p*DFB (B3LYP/aug-cc-pVTZ), labelled using the D_i notation in the present work. See text for details.

Figure 5: Variation in vibrational wavenumbers for symmetric *para*-disubstituted benzenes. The vibrations have been grouped into their C_{2v} symmetry groups: a_1 , a_2 , b_1 and b_2 . The lines arise from “iso” calculations taking the force field for *p*DFB and artificially varying the masses of the two fluorine atoms simultaneously from 15 to 127 amu. The symbols are the experimental values discussed in the text and given in Table 2. The high wavenumber C–H stretches, D_1 and D_2 (a_1 symmetry) and D_{21} and D_{22} (b_2 symmetry) are omitted for clarity.

Figure 6: Generalised Duschinsky matrix showing how the vibrational modes of *p*Xyl, using the *p*DFB force field, and changing the mass of both fluorine atoms to 15 amu, and the using explicitly calculated asymmetric *p*-dihalobenzenes wavefunctions can be expressed in terms of the *p*DFB ones. Black shading indicates a normalized coefficient value of 1.00, while white indicates a value of 0.00, with grey shading indicating intermediate values, see text for details.

Figure 7: Variation in vibrational wavenumbers for asymmetric *para*-disubstituted benzenes. The vibrations have been grouped into their C_{2v} symmetry groups: a_1 , a_2 , b_1 and b_2 . The lines arise from “iso” calculations taking the force field for *p*DFB and artificially varying the mass of the *para* fluorine atom from 15 to 127 amu. The symbols are the experimental values discussed in the text and given in Table 3. The high wavenumber C–H stretches, D_1 and D_2 (a_1 symmetry) and D_{21} and D_{22} (b_2 symmetry) are omitted for clarity.

Figure 8: Generalised Duschinsky matrix showing how the vibrational modes of *p*FT, using the *p*DFB force field, and changing the mass of one fluorine atom to 15 amu, and the using explicitly calculated asymmetric *p*-dihalobenzenes wavefunctions can be expressed in terms of the *p*DFB ones. Black shading indicates a normalized coefficient value of 1.00, while white indicates a value of 0.00, with grey shading indicating intermediate values, see text for details.

Figure 9: Calculated vibrational modes for four of the *p*-FIB (B3LYP/aug-cc-pVTZ) modes, labelled using the D_i notation in the present work. See text for details. The iodine atom is represented by the larger black circle, and the fluorine atom by the smaller black circle. Because of the asymmetry of the masses of the halogen atoms, these two pairs evolve into localized modes from the in-phase and out-of-phase analogues of *p*DFB – see text for further discussion.

Figure 10: Variation in vibrational wavenumbers for the *p*-halotoluenes and *p*-cresol. The vibrations have been grouped into their C_{2v} symmetry groups: a_1 , a_2 , b_1 and b_2 – see text for further discussion. The lines arise from “iso” calculations taking the force field for *p*DFB and changing the mass of the *ipso*-fluorine to 15 and artificially varying the mass of the *para*-fluorine atom from 15 to 127 amu. The symbols are the experimental values discussed in the text and given in Table 4. The high wavenumber C–H stretches, D_1 and D_2 (a_1 symmetry) and D_{21} and D_{22} (b_2 symmetry) are omitted for clarity.

Figure 11: Variation in vibrational wavenumbers for the *p*-halophenols, hydroquinone and *p*-cresol. The vibrations have been grouped into their C_{2v} symmetry groups: a_1 , a_2 , b_1 and b_2 – see text for further discussion. The lines arise from “iso” calculations by taking the force field for *p*DFB and changing the mass of the *ipso*-fluorine to 17 and artificially varying the mass of the *para*-fluorine atom from 15 to 127 amu. The symbols are the experimental values discussed in the text and given in Table 5. The high wavenumber C–H stretches, D_1 and D_2 (a_1 symmetry) and D_{21} and D_{22} (b_2 symmetry) are omitted for clarity.

Figure 1:

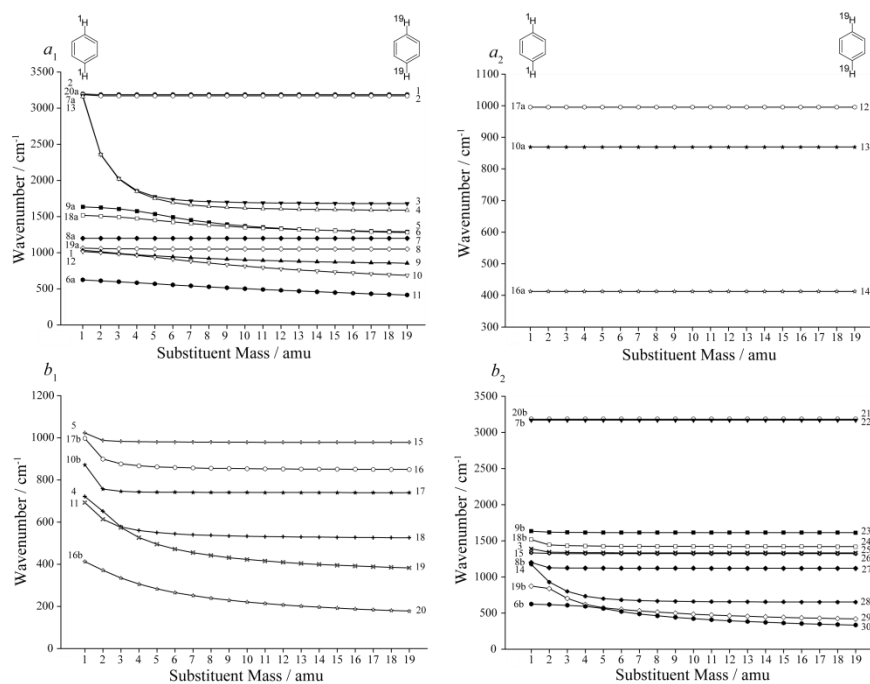


Figure 2

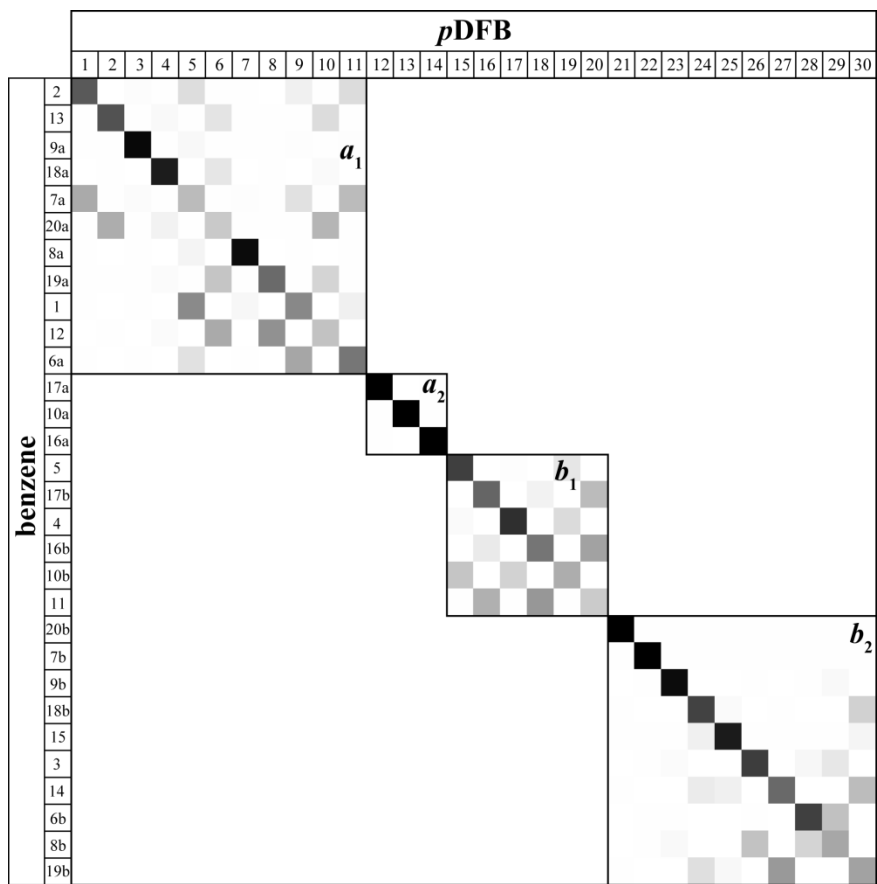


Figure 3

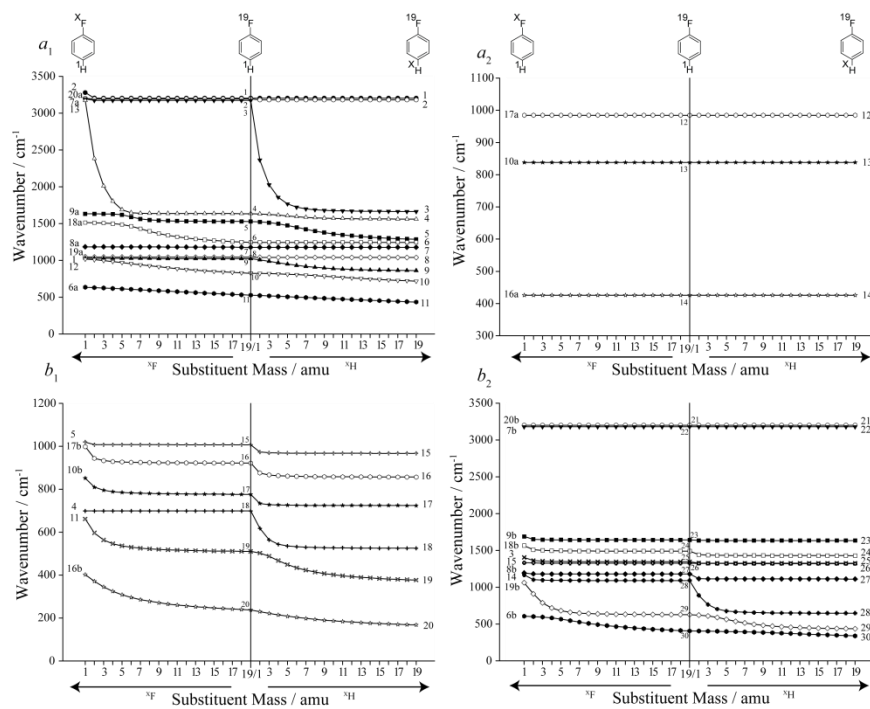


Figure 4:

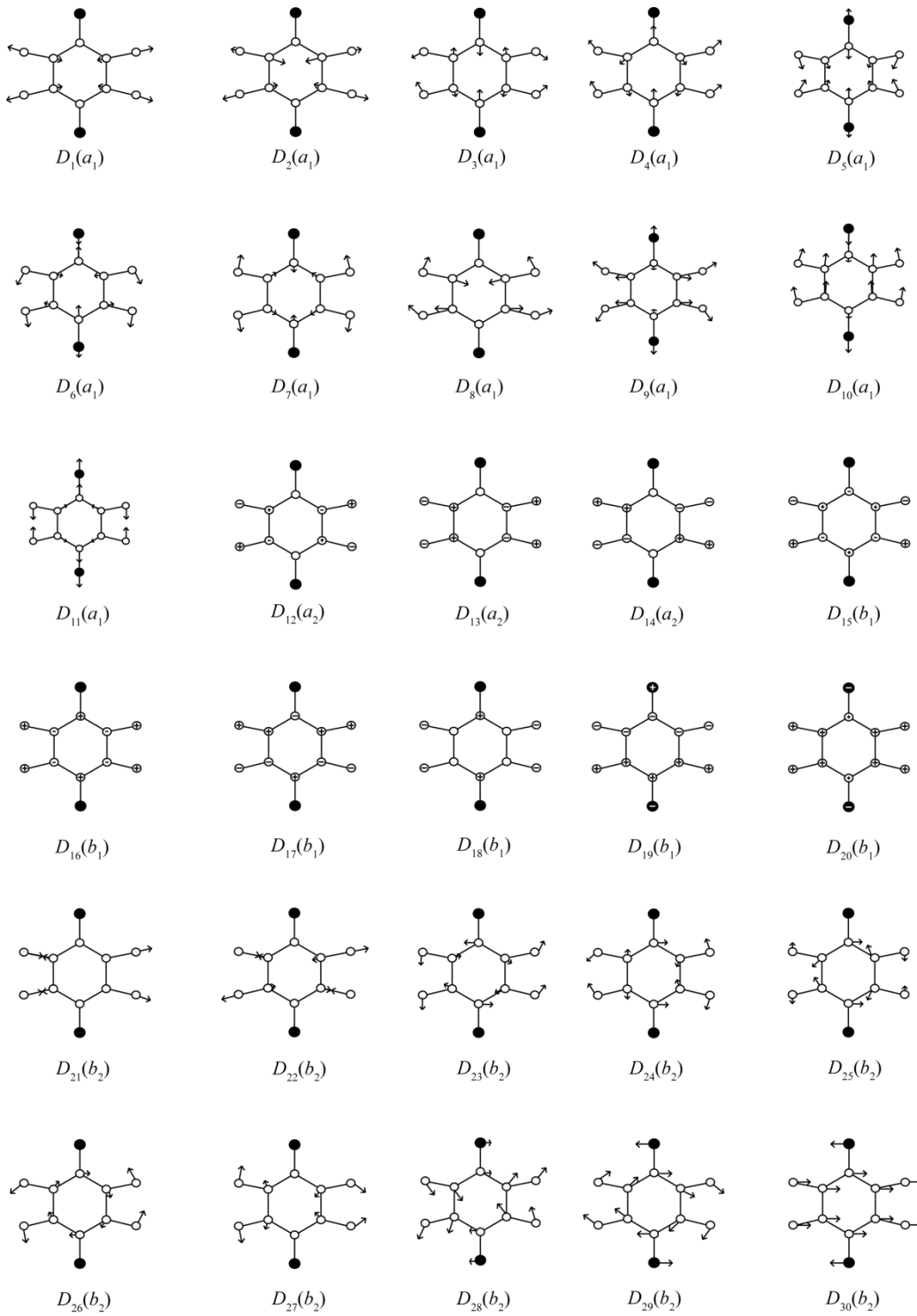


Figure 5:

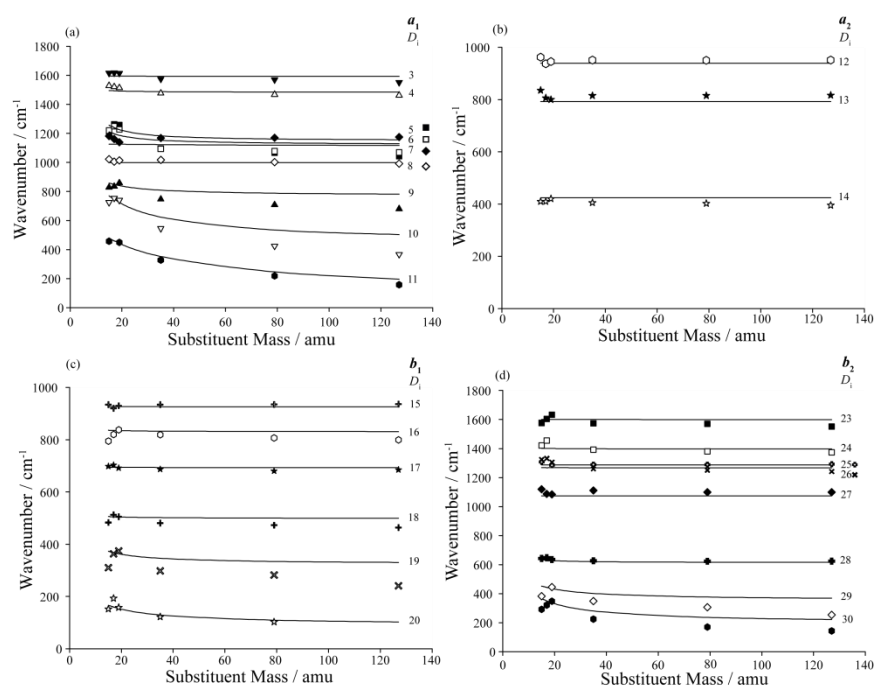


Figure 6

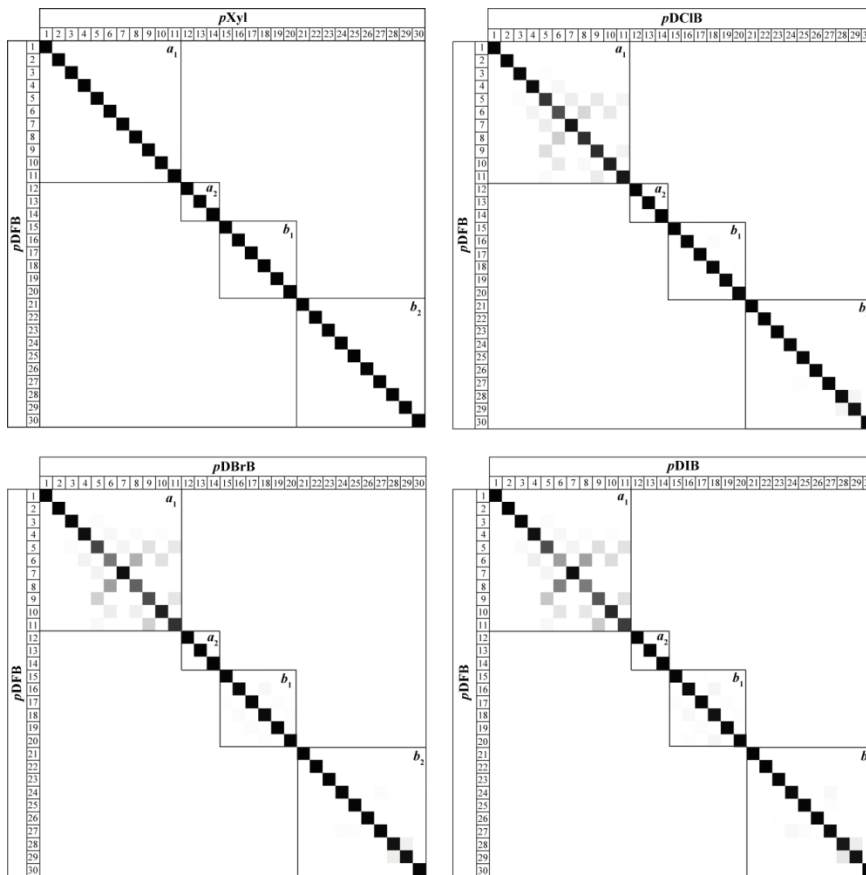


Figure 7:

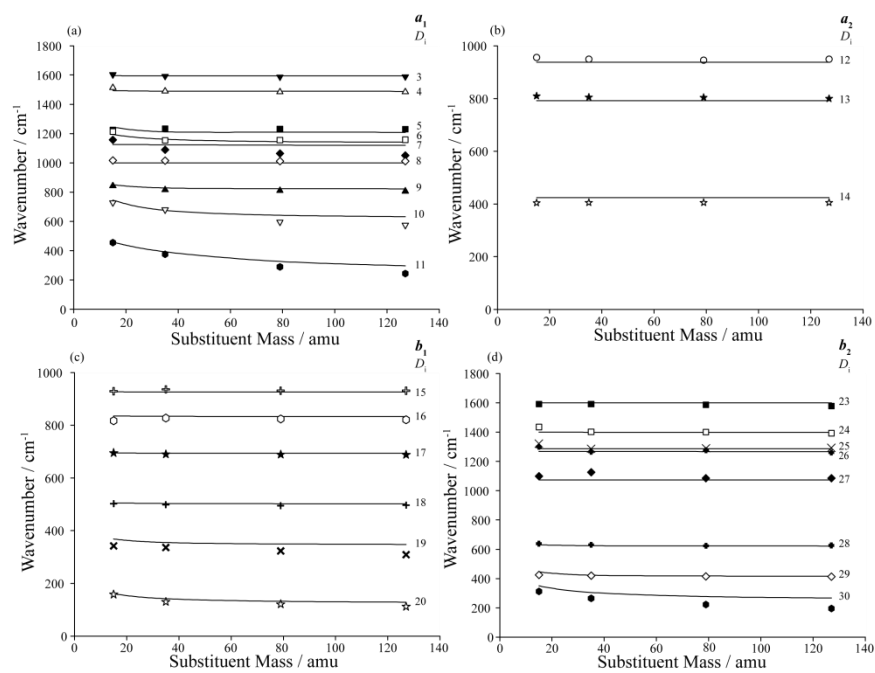


Figure 8:

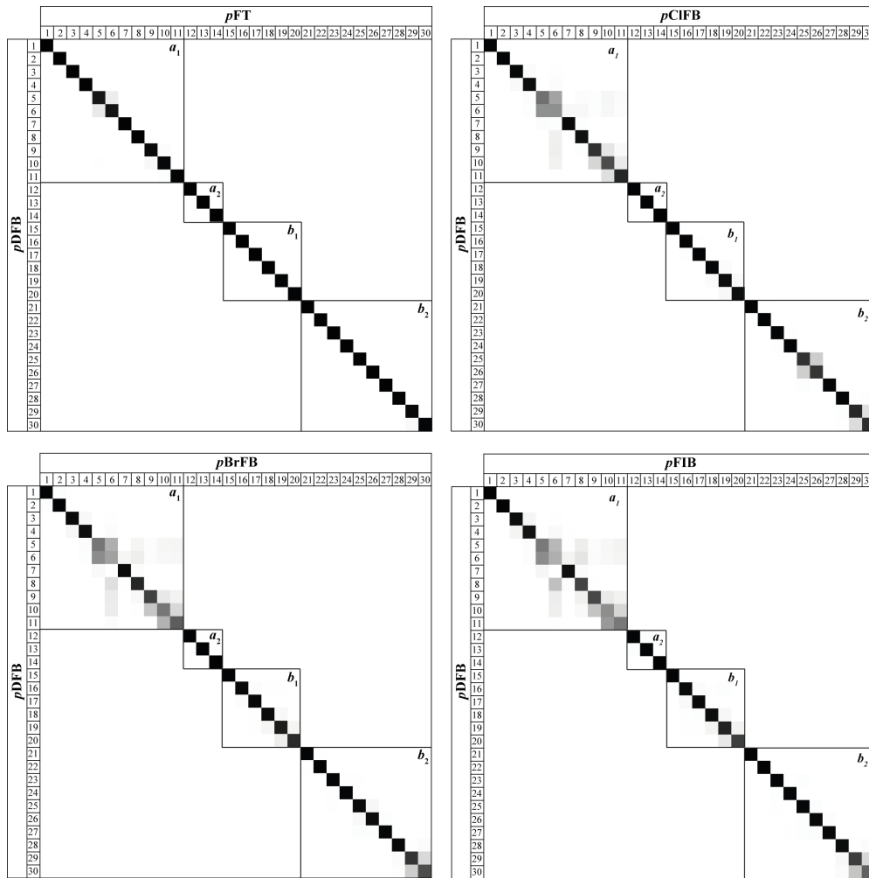
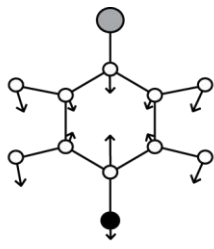
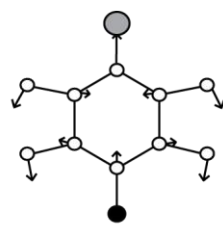


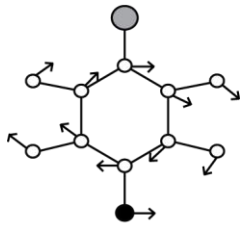
Figure 9:



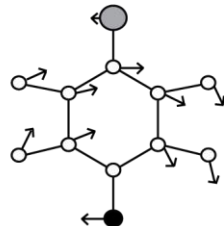
$D_5(a_1)$



$D_6(a_1)$



$D_{29}(b_2)$



$D_{30}(b_2)$

Figure 10:

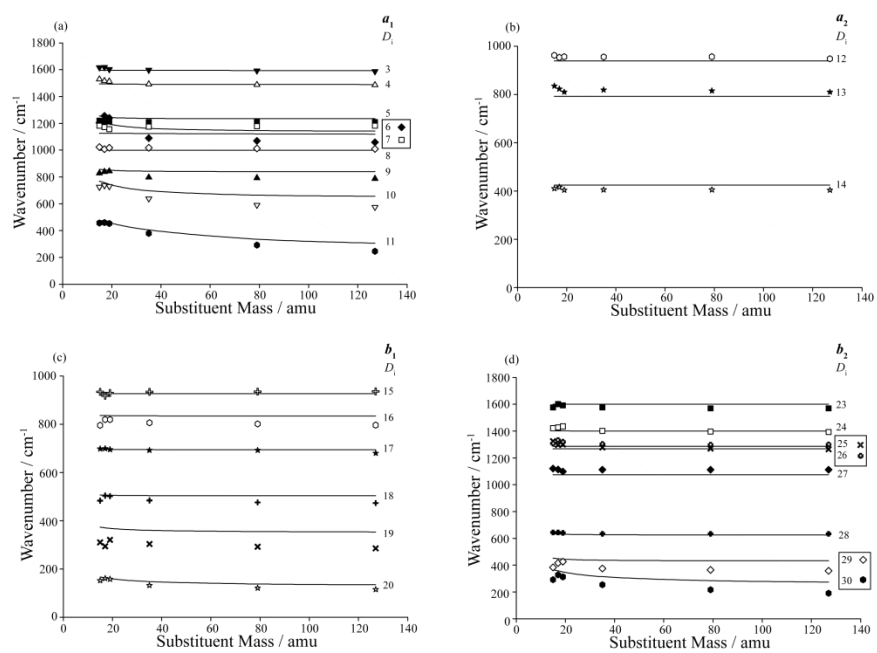
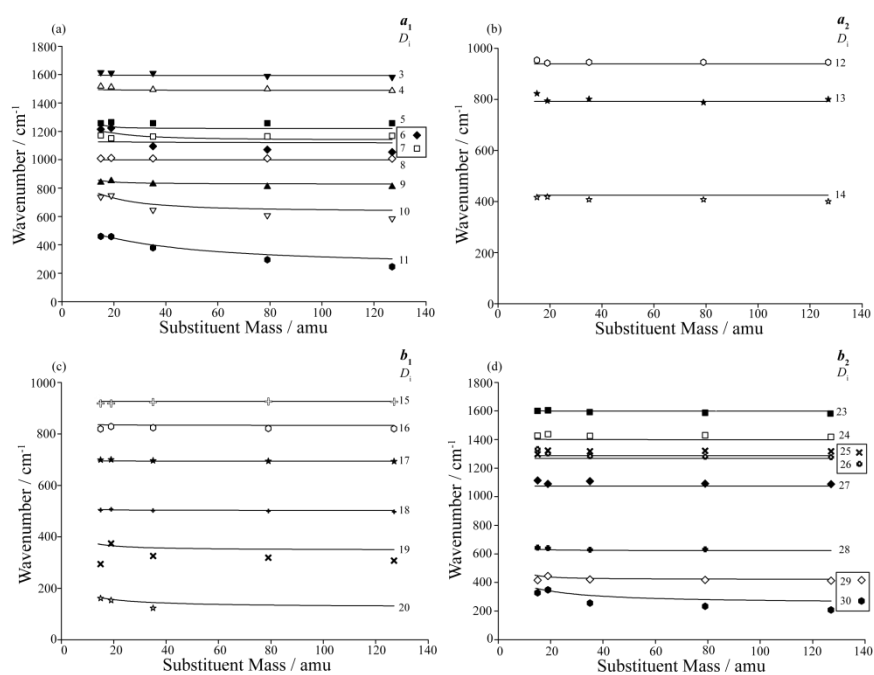


Figure 11:



References

-
- ¹ E. B. Wilson, Jr, Phys. Rev. 45 (1934) 706.
- ² A. M. Gardner and T. G. Wright. J. Chem. Phys. 135 (2011) 114305.
- ³ I. Pugliesi, N. M. Tonge, and M. C. R. Cockett, J. Chem. Phys. 129 (2008) 104303.
- ⁴ P. Butler, D. B. Moss, H. Yin, T. W. Schmidt and S. H. Kable, J. Chem. Phys. 127 (2007) 094303.
- ⁵ G. Varsányi, *Assignments of the Vibrational Spectra of Seven Hundred Benzene Derivatives* (Wiley, New York, 1974).
- ⁶ J. P. Harris, A. Andrejeva, W. D. Tuttle, I. Pugliesi, C. Schriever and T. G. Wright J. Chem. Phys. 141 (2014) 244315.
- ⁷ A. Andrejeva, W. D. Tuttle, J. P. Harris and T. G. Wright J. Chem. Phys. 143 (2015) 104312.
- ⁸ A. Andrejeva, W. D. Tuttle, J. P. Harris and T. G. Wright J. Chem. Phys. accepted (2016). [<http://dx.doi.org/10.1063/1.4938501>]
- ⁹ R. S. Mulliken, J. Chem. Phys. 23 (1955) 1997.
- ¹⁰ G. Herzberg, *Molecular Spectra and Molecular Structure II: Infrared and Raman Spectra of Polyatomic Molecules* (Krieger, Malabar, 1991), p.272.
- ¹¹ *Gaussian 09*, Revision C.01, M. J. Frisch, G. W. Trucks, H. B. Schlegel, G. E. Scuseria, M. A. Robb, J. R. Cheeseman, G. Scalmani, V. Barone, B. Mennucci, G. A. Petersson, H. Nakatsuji, M. Caricato, X. Li, H. P. Hratchian, A. F. Izmaylov, J. Bloino, G. Zheng, J. L. Sonnenberg, M. Hada, M. Ehara, K. Toyota, R. Fukuda, J. Hasegawa, M. Ishida, T. Nakajima, Y. Honda, O. Kitao, H. Nakai, T. Vreven, J. A. Montgomery, Jr., J. E. Peralta, F. Ogliaro, M. Bearpark, J. J. Heyd, E. Brothers, K. N. Kudin, V. N. Staroverov, R. Kobayashi, J. Normand, K. Raghavachari, A. Rendell, J. C. Burant, S. S. Iyengar, J. Tomasi, M. Cossi, N. Rega, J. M. Millam, M. Klene, J. E. Knox, J. B. Cross, V. Bakken, C. Adamo, J. Jaramillo, R. Gomperts, R. E. Stratmann, O. Yazyev, A. J. Austin, R. Cammi, C. Pomelli, J. W. Ochterski, R. L. Martin, K. Morokuma, V. G. Zakrzewski, G. A. Voth, P. Salvador, J. J. Dannenberg, S. Dapprich, A. D. Daniels, Ö. Farkas, J. B. Foresman, J. V. Ortiz, J. Cioslowski, and D. J. Fox, Gaussian, Inc., Wallingford CT, 2009.
- ¹² A. M. Gardner, A. M. Green, V. M. Tame-Reyes, V. H. K. Wilton and T. G. Wright, J. Chem. Phys. 138 (2013) 134303.
- ¹³ A. M. Gardner, A. M. Green, V. M. Tame-Reyes, K. L. Reid, J. A. Davies, V. H. K. Parkes and T. G. Wright, J. Chem. Phys. 140 (2014) 114038.

-
- ¹⁴ I. Pugliesi and K. Muller-Dethlefs, *J. Phys. Chem. A*, **110**, 4657 (2006), a free download of the software can be found at <http://www.fclab2.net>
- ¹⁵ R. L. Zimmerman and T. M. Dunn, *J. Mol. Spec.* 110 (1985) 312.
- ¹⁶ A. F. Childs, T. M. Dunn, and A. H. Francis, *J. Mol. Spec.* 102 (1983) 56.
- ¹⁷ A. A. Jarzęcki, E. R. Davidson, Q. Ju and C. S. Parmenter, *Int. J. Quant. Chem.* 72 (1999) 249.
- ¹⁸ M. J. Robey and E. W. Schlag, *Chem. Phys.* 30 (1978) 9.
- ¹⁹ A. E. W. Knight and S. H. Kable, *J. Chem. Phys.* 89 (1988) 7139.
- ²⁰ S. Saėki, *Bull Chem. Soc. Japan* 35 (1962) 326.
- ²¹ J. R. Scherer and J. C. Evans, *Spectrochim. Acta* 19 (1963) 1739.
- ²² J. H. S. Green, *Spectrochimica Acta A*, 26 (1970) 1503.
- ²³ A. Stojiljković and D. H. Whiffen, *Spectrochim. Acta* 12, (1958) 47.
- ²⁴ E. Herz, K. W. F. Kohlrausch and R. Vogel, *Monats. Chem.* 76 (1947) 200-214.
- ²⁵ P. R. Griffiths and H. W. Thompson, *Proc. R. Soc. London A* 298 (1967) 51.
- ²⁶ J. A. Draeger, *Spectrochimica Acta A* 41 (1985) 607.
- ²⁷ J. I. Selco and P. G. Carrick, *J. Mol. Spect.* **173**, 262 (1995).
- ²⁸ A. Hidalgo and C. Otero, *Spectrochim. Acta* 16 (1960) 528.
- ²⁹ R. J. Jakobsen and E. J. Brewer, *Appl. Spectrosc.* 16 (1962) 32.
- ³⁰ H. Wilson, *Spectrochim. Acta A* 30 (1974) 2141.
- ³¹ K. Fukushima and M. Sakurada, *J. Phys. Chem.* 80 (1976) 1367.
- ³² M. Kubinyi and G. Keresztury, *Spectrochim. Acta A* 45 (1989) 421.
- ³³ M. Kubinyi, F. Billes, A. Grofcsif and G. Keresztury, *J. Molec. Struct.* 266 (1992) 339.
- ³⁴ N. A. Narasimham, M. Z. El-Sabban and J. R. Nielsen, *J. Chem. Phys.* 24 (1956) 420.
- ³⁵ N. D. Patel, V. B. Kartha and N. A. Narasimham, *J. Mol. Spec.* 48, (1973) 202.
- ³⁶ N. D. Patel, V. B. Kartha and N. A. Narasimham, *J. Mol. Spec.* 48 (1973) 185.
- ³⁷ S. K. Singh and K. N. Upadhya, *Pramāṇa* 14 (1980) 389.
- ³⁸ A. Stojiljković and D. H. Whiffen, *Spectrochim. Acta* 12, (1958) 57.
- ³⁹ O. Paulsen, *Monatsh. Chem.* 72 (1939) 244.
- ⁴⁰ K. W. F. Kohlrausch and A. Pongratz, *Monatsh. Chem.* 65 (1934) 199.
- ⁴¹ C. Pal and P. N. Ghosh, *J. Mol. Spec.* 172 (1995) 102.
- ⁴² P. N. Ghosh, *J. Mol. Spec.* 142, (1990) 295.
- ⁴³ Y. M. Ha, L. S. Choi and S. K. Lee, *Bull. Korean Chem. Soc.* 19 (1998) 202.
- ⁴⁴ C. J. Seliskar, M. A. Leugers, M. Heaven, and J. L. Hardwick, *J. Mol. Spec.* 106 (1984) 330.
- ⁴⁵ K. Okuyama, N. Mikami and M. Ito, *J. Phys. Chem.* 89 (1985) 5617.

-
- ⁴⁶ T. Ichimura, K. Nahara, Y. Mori, M. Sumitani and K. Yoshihara, *Chem. Phys.* 95, (1985) 9.
- ⁴⁷ H. Kojima, T. Suzuki, T. Ichimura, A. Fujii, T. Ebata and N. Mikami, *J. Photochem. Photobiol. A: Chem.* 90, (1995) 1.
- ⁴⁸ W. J. Balfour and D. Ristic-Petrovic, *J. Phys. Chem.* 97 (1993) 11643.
- ⁴⁹ J. H. S. Green, D. J. Harrison and W. Kynaston, *Spectrochim. Acta A* 27, (1971) 2199.
- ⁵⁰ P. Biswas, P. Pandey and T. Chakraborty, *Chem. Phys. Lett.* 454 (2008) 163.
- ⁵¹ W. Zierkiewicz, D. Michalska, B. Czarnik-Matuszewicz and M. Rospenk, *J. Phys. Chem. A* 107 (2003) 4547.
- ⁵² P. Imhof and K. Kleinermanns, *Phys. Chem. Chem. Phys.* 4 (2002) 264.
- ⁵³ W. Zierkiewicz, D. Michalska and T. Zeegers-Huyskens, *J. Phys. Chem. A* 104 (2000) 11685.
- ⁵⁴ Z. Arp, D. Autrey, J. Laane, S. A. Overman and G. J. Thomas, Jr. *Biochemistry* 40 (2001) 2522.
- ⁵⁵ R. J. Jakobsen, *Spectrochim. Acta* 21 (1965) 433.